PL-TR-93-2185
Environmental Research Papers, No. 1128

ATMOSPHERIC STRUCTURE SIMULATION: AN AUTOREGRESSIVE MODEL FOR SMOOTH GEOPHYSICAL POWER SPECTRA WITH KNOWN AUTOCORRELATION FUNCTION

James H. Brown

5 February 1993

PHILLIPS LABORATORY
Directorate of Geophysics
AIR FORCE MATERIEL COMMAND
HANSCOM AIR FORCE BASE, MA 01731-3010

"This technical report has been reviewed and is approved for publication"

William Blumberg
Simulations Branch
Branch Chief

Roger VanTassel
Optical Environment Division
Division Director

This report has been reviewed by the ESC Public Affairs Office (PA) and is releasable to the National Technical Information Service (NTIS)

Qualified requestors may obtain additional copies from the Defense Technical Information Center. All others should apply to the National Technical Information Service.

If your address has changed, or if you wish to be removed from the mailing list, or if the addressee is no longer employed by your organization, please notify PL/TSI, Hanscom AFB, MA 01731-3010 This will assist us in maintaining a current mailing list.

Do not return copies of this report unless contractual obligations or notices on a specific document requires that it be returned.

REPORT DOCUMENTATION PAGE

Form Approved
OMB No. 0704-0188

1. AGENCY USE ONLY *(Leave blank)*	2. REPORT DATE	3. REPORT TYPE AND DATES COVERED
	5 FEBRUARY 1993	Scientific Interim 1Oct91-20Jan93

4. TITLE AND SUBTITLE
Atmospheric Structure Simulation:
An Autoregressive Model For Smooth Geophysical Power Spectra With Known Autocorrelation Function

5. FUNDING NUMBERS
Project: S311
Task: S31105
WU: S3110501
PE: 63215C
Related IHWUS : S3211301
and 3054GD04

6. AUTHOR(S)
James H. Brown

7. PERFORMING ORGANIZATION NAME(S) AND ADDRESS(ES)
Phillips Laboratory(GPOS)
29 Randolph Road
Hanscom AFB, MA 01731-3010

8. PERFORMING ORGANIZATION REPORT NUMBER
PL-TR-93-2185
ERP, NO. 1128

9. SPONSORING/MONITORING AGENCY NAME(S) AND ADDRESS(ES)

10. SPONSORING/MONITORING AGENCY REPORT NUMBER

11. SUPPLEMENTARY NOTES

12a. DISTRIBUTION/AVAILABILITY STATEMENT
Approved for public release; distribution unlimited

12b. DISTRIBUTION CODE

13. ABSTRACT *(Maximum 200 words)*

Within a defined domain, geophysical phenomena often are characterized by smooth continuous power spectral densities having a negative power law slope. Frequently, Fourier transform analysis has been employed to generate synthetic scenes from pseudorandom arrays by passing the stochastic data through a Fourier filter having a desired correlation structure and power spectral dependency. This report examines the possibility of producing synthetic structure by invoking autoregression analysis as contrasted with the Fourier method. Since computations that apply multidimensional fast Fourier transforms to large data arrays consume enormous resources and time, the goal of this study is to seek an alternative method to reduce the computational burden. Future editions of the Phillips Laboratory Strategic High Altitude Atmospheric Radiance Code (SHARC) will feature an ability to calculate structured radiance. The methods explored herein provide a process that can complement or in some cases supplement methods presently being used.

14. SUBJECT TERMS
Power spectra, PSD, Spectral analysis, Autoregression, Fourier transform, SHARC, Structure, Structure simulation.

15. NUMBER OF PAGES
62

16. PRICE CODE

17. SECURITY CLASSIFICATION OF REPORT	18. SECURITY CLASSIFICATION OF THIS PAGE	19. SECURITY CLASSIFICATION OF ABSTRACT	20. LIMITATION OF ABSTRACT
Unclassified	Unclassified	Unclassified	SAR

Contents

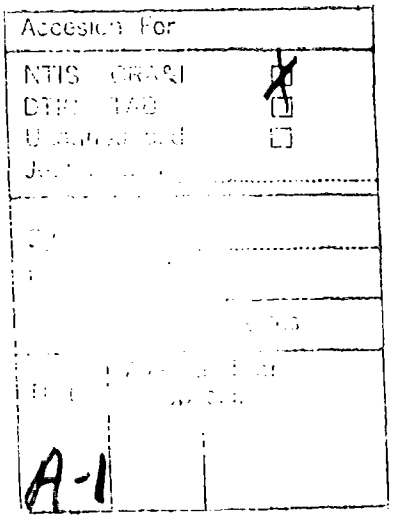

Illustrations

Acknowledgment

The author gratefully acknowledges the contributions of Neil Grossbard for the computer programs, computer runs, graphics, and insights into the mathematical analysis that helped make this report possible.

Atmospheric Structure Simulation: An Autoregressive Model For Smooth Geophysical Power Spectra With Known Autocorrelation Function

1. INTRODUCTION

Atmospheric fluctuations in wind speed and gravity waves are characterized by continuous power spectral density functions. For example, one dimensional wind speed PSD's are found to have log-log slopes of about -5/3. Such spectra often are used in simulating an environment or predicting atmospheric structure. Fast Fourier transform analysis provides a means for filtering white noise with spatial filters to simulate a stationary time or spatial data set. In many applications the transform technique provides adequate processing speed. For example, repeatedly using the double precision IMSL routine DF2TCF, a [illegible] point transform averages 6.91 ms on the Phillips Laboratory Convex model 210 computer. Geophysical data however, are multidimensional, and often exceed 1024 points. Three dimensional Fourier simulation of atmospheric structure that realistically allows for variable coherence length scales, RMS fluctuation levels, and spectral slopes would require months of execution time on a work station.

The Phillips Laboratory Strategic High Altitude Atmospheric Radiance Code (SHARC)[1] uses first principles to calculate point-to-space and limb viewing atmospheric background infrared radiance and transmittance. Real atmospheric infrared background perturbations occur from fluctuations in temperature and density of the contributing molecular species. Version 4 of the SHARC code envisions a capability to evaluate radiance structure from estimated variances in the standard temperature and density profiles. To provide a realistic but practical two-dimensional structure scene capability will require creative, efficient, and tested algorithms. The purpose of this report is to study the possibility of producing synthetic structure from autoregression analysis as contrasted with the common Fourier method with a view toward reducing the

Received for publication 4 February 1993

[1]Sharma, R.D., et.al., (1991) *Description of SHARC-2, The Strategic High Altitude Atmospheric Radiance Code*, Phillips Laboratory technical report, PL-TR-91-2071, ADA 239008

computational burden. Only one-dimensional analysis is treated here but a subsequent report will present a two-dimensional approach.

2. THEORY OF AUTOREGRESSIVE DIGITAL SPECTRAL ESTIMATION

This section is a brief review of autoregressive digital spectral estimation as presented by S. Lawrence Marple[2] and Steven M. Kay[3].

An autoregressive moving average (ARMA) model for a discrete time series, x(n), that approximates deterministic and stochastic processes can be represented by the filter linear difference equation:

$$x(n) = -\sum_{k=1}^{p} a(k)x(n-k) + \sum_{k=0}^{q} b(k)\varepsilon(n-k)$$

in which $x(n)$ is the output sequence and $\varepsilon(n)$ a white noise input driving sequence. The a(k) and b(k) coefficients form the autoregressive and moving average portions of the ARMA model respectively. A z transform analysis of the difference equation shows that the ARMA power spectral density (PSD) is:

$$P_{ARMA}(f) = T\rho_w \left| \frac{B(f)}{A(f)} \right|^2$$

where,

$$A(f) = 1 + \sum_{k=1}^{p} a(k) \exp(-2\pi i f k T)$$

and,

$$B(f) = 1 + \sum_{k=1}^{q} b(k) \exp(-2\pi i f k T).$$

T is the sampling interval and ρ_w is the variance of the white noise process. If all the moving average coefficients are zero, except b(0) = 1, then

$$x(n) = -\sum_{k=1}^{p} a(k)x(n-k) + \varepsilon(n)$$

and the process is strictly autoregressive of order p. The autoregressive PSD becomes,

---

[2]Marple, S.L., 1987 *Digital Spectral Analysis with Applications*, Chapter 6, Prentice-Hall, Englewood Cliffs, New Jersey.

[3]Kay, Steven M., 1988 *Modern Spectral Estimation, Theory & Application*, Prentice-Hall, Englewood Cliffs, New Jersey.

$$P_{AR}(f) = \frac{T\rho_w}{|A(f)|^2} = T\sum_{k=-\infty}^{\infty} r_{xx}(k)\exp(-2\pi ifkT)$$

where r_{xx} is the autocorrelation sequence at k and ρ_w is the variance of $\varepsilon(n)$. The relationship between the autocorrelation sequence and the pure autoregressive model is

$$r_{xx}(m) = \begin{cases} -\sum_{k=1}^{p} a(k) r_{xx}(m-k) & \text{for } m > 0 \\ -\sum_{k=1}^{p} a(k) r_{xx}(-k) + \rho_w & \text{for } m = 0 \\ r_{xx}^*(-m) & \text{for } m < 0 \end{cases}$$

This expression may be evaluated for the p+1 lag indices $0 \le n \le p$ by:

$$\begin{pmatrix} r_{xx}(0) & r_{xx}(-1) & \cdots & r_{xx}(-p) \\ r_{xx}(1) & r_{xx}(0) & \cdots & r_{xx}(a(1)) \\ \vdots & \vdots & \ddots & \vdots \\ r_{xx}(p) & r_{xx}(p-1) & \cdots & r_{xx}(0) \end{pmatrix} \begin{pmatrix} 1 \\ a(1) \\ \vdots \\ a(p) \end{pmatrix} = \begin{pmatrix} \rho_w \\ 0 \\ \vdots \\ 0 \end{pmatrix}$$

This expression forms the autoregressive Yule-Walker equations. Given the autocorrelation sequence for lags 0 to p, the autoregressive coefficients may be found from the above. Since $r_{xx}(-k) = r^*_{xx}(k)$, the autocorrelation matrix is both Toeplitz and Hermitian. A standard "Levinson" algorithm, which takes advantage of the Hermitian-Toeplitz matrix equation, was employed to solve for the AR parameters. The same Yule-Walker equations also occur if we attempt to solve the problem: find the "best", in a least square sense, set of equations that determine the coefficients that predict $\hat{X}$ from $\hat{x}(n) = -\sum_{k=1}^{p} a(k)x(n-k)$, where $\overline{(\hat{x}(n) - x(n))^2} = \rho_w$. In summary, the Levinson recursion computes sets of coefficients $\{a_1(1), \rho_1\}$, $\{a_2(1), a_2(2), \rho_2\}$, ..., $\{a_p(1), a_p(2), \ldots, a_p(p), \rho_p\}$ where the final set at order p is the desired solution of the Yule-Walker expressions. For the AR(p) process, $a_p(i) = a(i)$ for i = 1, 2, 3, ..., p and ρ_p is the minimum prediction error, that is, $\rho_w = \rho_p = \rho_{min} = \xi\left[x^*[n]\left(x[n] - \hat{x}[n]\right)\right]$. The algorithm is initialized by:

$$a_1[1] = -\frac{r_{xx}[1]}{r_{xx}[0]}$$

$$\rho_1 = \left(1 - |a_1[1]|^2\right) r_{xx}[0]$$

with the recursion for k = 2, 3, ..., p given by

$$a_k[k] = -\frac{r_{xx}[k] + \sum_{\ell=1}^{k-1} a_{k-1}[\ell] r_{xx}[k-\ell]}{\rho_{k-1}}$$

$$a_k[i] = a_{k-1}[i] + a_k[k] a_{k-1}^*[k-i] \quad i = 1, 2, \ldots, k-1$$

$$\rho_k = \left(1 - |a_k[k]|^2\right) \rho_{k-1}$$

The $a_k[k]$ coefficients are known as reflection coefficients.

3. APPLICATION TO ATMOSPHERIC POWER SPECTRAL DENSITIES

Atmospheric power spectral density functions often are modeled by power law functions of the form[4,5]

$$PSD(k) = \frac{C}{\left(a^2 + k^2\right)^{\nu + 1/2}}$$

The constant C is found from the definition that the total variance of the associated time series, σ^2, is equal to the area under the PSD[6],

$$\sigma^2 = 2\int_0^\infty PSD(k)dk = 2C\int_0^\infty \frac{dk}{\left(a^2 + k^2\right)^{\nu + 1/2}} = 2C\frac{\sqrt{\pi}\Gamma(\nu)}{2a^{2\nu}\Gamma\left(\nu + \frac{1}{2}\right)}$$

so that the PSD model is

$$PSD(k) = \frac{\sigma^2 a^{2\nu}\Gamma\left(\nu + \frac{1}{2}\right)}{\sqrt{\pi}\Gamma(\nu)\left(a^2 + k^2\right)^{\nu + 1/2}}$$

The relationship between the frequency domain PSD and the time or spatial domain autocorrelation function is specified by their Fourier transform pairs. Thus the autocorrelation function, (ACF), for the real even PSD function is

---

[4]Tatarski, V.I., 1961 *Wave Propagation in a Turbulent Medium*. McGraw-Hill, .

[5]Futterman, W.I., Schweitzer, E.L., and Newt, J.E. 1991 "Estimation of Scene Correlation Lengths", Characterization, Propagation, and Simulation of Sources and Backgrounds, *Proceedings SPIE* - The International Society of Optical Engineering, V1486, pp127-140, Orlando, Florida.

[6]For the integral, see for example, Gradshteyn, I.S. and Ryzhik, I.M., 1965 *Table of Integrals Series and Products*, eq 3.241.4, Academic Press.

$$ACF(x) = IFFT(PSD) = 2\int_0^\infty \frac{\sigma^2\Gamma\left(\nu+\frac{1}{2}\right)a^{2\nu}\cos(2\pi xk)dk}{\sqrt{\pi}\Gamma(\nu)\left(a^2+k^2\right)^{\nu+1/2}}$$

The integral is evaluated using the Bessel function of the second kind of fractional order, K_ν to be[7]

$$ACF(x) = \frac{\sigma^2 2^{(1-\nu)}(2\pi ax)^\nu K_\nu(2\pi ax)}{\Gamma(\nu)}$$

Expressions for two and three dimensional power spectral densities can be evaluated from the model autocorrelation function by performing two and three dimensional Fourier transforms of ACF(x). For example, over the valid range for ν, the two-dimensional isotropic power spectral density is

$$F(\vec{k}) = \frac{1}{(2\pi)}\iint \cos(\vec{k}\cdot\vec{r})ACF(\vec{r})d\vec{r}$$

$$F(f_k) = \frac{\sigma^2\nu a^{2\nu}}{\pi\left(a^2+f_k^2\right)^{\nu+1}}$$

while the three-dimensional isotropic power spectral density is

$$\Phi(\vec{k}) = \frac{1}{(2\pi)^3}\iiint \cos(\vec{k}\cdot\vec{r})ACF(\vec{r})d\vec{r}$$

$$\Phi(f_k) = \frac{\Gamma\left(\nu+\frac{3}{2}\right)\sigma^2 a^{2\nu}}{\pi\sqrt{\pi}\Gamma(\nu)\left(a^2+f_k^2\right)^{\nu+3/2}}$$

The parameter "a" can be expressed in terms of the integral scale or equivalent width of the ACF. An equivalent width is defined as the area of a function divided by its central ordinate[8], or

$$\frac{\int_{-\infty}^{\infty} f(x)dx}{f(0)}$$

Thus the large scale correlation length L_c is defined by integrating ACF(x) over all positive values of x.

$$L_c = \frac{\int_0^\infty ACF(x)dx}{\sigma^2}$$

---

[7]Ibid., Eq 8 -32.5

[8]Bracewell, R.N., 1978 *The Fourier Transform and Its Applications*, McGraw-Hill, New York.

where σ^2 is the autocorrelation at zero separation. Observing that the equivalent width of a function is equal to the inverse of the equivalent width of its transform[9], the correlation length may be written as

$$L_c = \frac{PSD(0)}{2\int_0^\infty PSD(k)dk} = \frac{PSD(0)}{2\sigma^2}$$

so that,

$$L_c = \frac{\sigma^2\Gamma\left(\nu+\frac{1}{2}\right)a^{2\nu}}{2\sigma^2\sqrt{\pi}\Gamma(\nu)a^{2\nu+1}} = \frac{\Gamma\left(\nu+\frac{1}{2}\right)}{2\sqrt{\pi}\Gamma(\nu)a} \quad or$$

$$a^{-1} = \frac{2\sqrt{\pi}\Gamma(\nu)}{\Gamma\left(\nu+\frac{1}{2}\right)}L_c$$

These relationships are visually compared in Figure 1. The upper left quadrant of the graph shows a log-log plot of the PSD function for a slope of -3, $\sigma^2 = 0.2$, $L_c = 5.0$ and $a = 0.05$. The upper right quadrant shows a linear plot of the PSD with L_c and σ^2 calculated from the curve. The autocorrelation function is plotted in the lower left quadrant and also shows L_c and σ^2 calculated from the curve. Quite obviously the parameter "a" depends upon the value of ν, such that "a" coincides with the "roll over" or "corner frequency" of the PSD. The correlation length, on the other hand, corresponds to a much higher frequency (and smaller PSD). As shown in the lower right quadrant of Figure 1, the parameter "a" assumes a value near the frequency of the peak power while $1/L_c$ assumes a value on the far tail of the power curve.

4. IMPLEMENTATION

In practice a given power law PSD was constructed from the PSD and ACF models:

$$PSD(f) = \frac{\sigma_r^2 a^{2\nu}\Gamma\left(\nu+\frac{1}{2}\right)}{\sqrt{\pi}\Gamma(\nu)\left(a^2+f^2\right)^{\nu+1/2}} \approx \frac{2\sigma_r^2\Delta x}{\left|1+\sum_{i=1}^{N} a_i e^{j2\pi f\Delta x}\right|^2}$$

$$ACF(x) = \frac{\sigma^2 2^{(1-\nu)}(2\pi a x)^\nu K_\nu(2\pi a x)}{\Gamma(\nu)}$$

---

[9] Ibid

where,

σ_r^2 = residual error

Δx = spacing

a_i = model parameters

$j = \sqrt{-1}$

f = frequency (Hz)

Then, a spatial data sequence was simulated using a normally distributed set of pseudorandom numbers G(J). The simulation of M sequence values proceeded as follows:

Set Y(1) = Y(2) = Y(3) = ··· =Y(N) = 0. Then for J = N+1, N+2, ···, M+1000, create Y(J) from

$Y(J) = G(J)\sigma_r - \sum_{i=1}^{N} a_i Y(J-i)$. The simulated sequence is then contained in Y(1001), Y(1002), ···, Y(M+1000).

After simulating such a discrete spatial sequence of a given PSD, the PSD of the simulated series was checked as follows. Using a forward and backward estimation method[10], a set of NN b_i coefficients were found to estimate the simulated PSD from the formula,

$$PSD(f) = \frac{2\sigma_e^2 \Delta x}{\left|1 + \sum_{i=1}^{NN} b_i e^{j2\pi f \Delta x}\right|^2}$$

where Δx is the same spacing used to generate the synthetic series.

The forward and backward method solves the following least squares problem. Given M discrete series values Y(J), for J = 1, 2, ···, M, we find b_i values that minimize ERR, where,

$$ERR = \left(\sum_{J=NN+1}^{M} \left(Y(J) - \sum_{i=1}^{NN} b_i Y(J-i) \right)^2 \right) + \left(\sum_{J=1}^{M-NN} \left(Y(J) - \sum_{i=1}^{NN} b_i Y(J+i) \right)^2 \right)$$

σ_e^2 is then equal to $\frac{ERR}{2(M-NN)}$.

5. RESULTS

[10]Haykin, Simon, ed., 1991 *Advances in Spectrum Analysis and Array Processing*. Vol. 1. Prentice Hall. Englewood Cliffs New Jersey. . pp.155-156.

The following discussion is aimed at producing a practical autoregressive model of atmospheric structure consistent with having a pre-assigned power spectral density and autocorrelation function. Correlation lengths and σ^2 variances are taken from Strugala, et.al.[11]

Figure 2 shows an 8000 point sequence of Gaussian "white noise" having a spacing of 100 m, mean of zero, and standard deviation of 0.055. Figure 3 presents a histogram of the Gaussian data and Figure 4 shows the "flat" white noise spectra and associated autocorrelation function. The theoretical and calculated statistics agree, with the calculated having an average of 0.000117 and σ of 0.0549. Correlated sequences, histograms, PSD's and ACF's of subsequent plots may be compared to this "unfiltered sequence."

Figure 5 is typical of all the plots in this report showing log-log PSD's in the left panel and ACF's in the right panel. This and subsequent plots have PSD's measured in $\frac{(\delta \text{ Temperature / Temperature})^2}{\text{Wavenumber}}$ and wavenumber measured in km^{-1}. Three curves usually appear in each panel. The solid unmarked curves are the "theoretical" or inputted PSD or ACF. The curves marked by an **X** are the autoregressive predicted PSD's and ACF's, and the curves marked by an open square are PSD's and ACF's derived from the simulated data sequences. Except where otherwise noted, the data spacing is 100 m and the Nyquist frequency is 5 km^{-1}. The input parameters for Figure 5 are L_c= 1.75 km, σ^2 = 0.00102, spectral slope (S) = -5/3. Using six linear predictor coefficients, the predicted values are L_c= 1.44 km from the PSD and 1.50 km from the ACF, and σ^2 = 0.00107 from the area of the PSD. Using 12 coefficients to determine the simulated results, the values for the simulated curves are L_c= 1.38 km from the PSD and 1.44 km from the ACF, and σ^2 = 0.00106 from the area of the PSD. Visually examining Figure 5, clearly shows that using 6 coefficients for the predictor and 12 coefficients for the simulated values reproduces the theoretical slope quite well except at the highest wavenumbers. Also, at low wavenumbers, the predicted and simulated PSD's show a ~16 percent DC bias from the theoretical. Part of the high wavenumber divergence is due to the sharpness of the autocorrelation function at zero lag. In fact, for the specified input spectral slope of -5/3, a sharp cusp exists at zero lag. This cusp introduces an error into the estimate of the linear prediction coefficients that affect the PSD at high wavenumbers. To test this hypothesis, the first value of the autocorrelation function at zero lag was modified by setting it equal to a value linearly extrapolated from the second and third values. This modification led to the curves in Figure 6. Here we see much better agreement between the theoretical and modeled curves at high wavenumbers and improvement at low wavenumbers. Improvement in the spectral parameters is also evident. L_c improves to 1.54 km for the predicted PSD and 1.60 km for the predicted ACF. Figure 7 shows a sequence of 8000 data points simulated over 800 km. When compared with Figure 2, the -5/3 spectral filtering is obvious. To see if the simulated data retains the Gaussian PDF, a histogram of the simulated data is examined in Figure 8. The figure shows that the variance of the simulated data = 0.00102, matching the input parameter, σ^2. Also, the histogram closely follows the shape of the theoretical PDF as shown by the solid curve. The effects of using more or fewer predictor coefficients are shown in Figures 9

---

[11] Strugala, L.A., Newt, J.E., Futterman, W.I., Schweitzer, E.L., Herman, B.J., and Sears, R.D. 1991 Development of High Resolution Statistically Non-stationary Infrared Earthlimb Radiance Scenes, *Characterization, Propagation, and Simulation of Sources and Backgrounds, Proceedings SPIE* - The International Society for Optical Engineering, V1486, pp 176-187, Orlando, Florida.

and 10. Figure 9 is calculated for only one predictor coefficient while Figure 10 is calculated using 20 predictor coefficients. Except for the bias at low wavenumbers, using only one coefficient for the predictor does remarkably well for the specified input parameters. However, with the use of 20 coefficients, any difference between the theoretical, predicted, and simulated curves is practically erased. Resultant values for the predicted and simulated spectral parameters also improve. For example, L_c improves to 1.63 km for the simulated PSD and 1.70 km for the simulated ACF. Figure 11 provides a visual perspective of how the 20 corresponding reflection coefficients decrease as a function of reflection coefficient number. Ordinarily, the reflection coefficient decreases smoothly and monotonically. However, introducing the modification to the ACF that was mentioned above causes the second reflection coefficient to dip below the smooth value. Evidently this helps compensate for the cusp in the ACF.

One may see the effects of increasing the value of the correlation length L_c, in Figures 12-14. These curves are calculated for L_c = 10 km, σ^2 = 0.0049, and S = -5/3. Using 6 coefficients for the predicted PSD and 12 coefficients for the simulated PSD, produces the curves of Figures 12 and 13. Figure 12 illustrates the increased difficulty in simulating a PSD and ACF having a large L_c with a small number of coefficients. Figure 13 clearly shows the effect of the larger correlation length on the simulated spatial sequence. As expected, greater smoothing (data correlation) results from using the larger scale size. Figure 14 illustrates the improvement in the predicted and simulated PSD and ACF by using 20 predictor coefficients for both the predicted and simulated curves.

Figures 15-20 show the result of repeating the calculations for a spectral slope of -2. Figures 15-17 have inputted spectral parameters of L_c = 1.75 and σ^2 = 0.00102 while Figures 18-20 have L_c = 10 and σ^2 = 0.0049. For a slope of -2, using 6 coefficients for the predicted PSD and 12 coefficients for the simulated PSD, gives good agreement between theoretical, predicted, and simulated curves, even for L_c = 10. For a theoretical L_c= 1.75, σ^2 = 0.00102, the predicted values are L_c= 1.73 from the PSD and 1.75 from the ACF, and σ^2 = 0.00104 from the area of the PSD. The values for the simulated curves are L_c= 1.65 from the PSD and 1.67 from the ACF, and σ^2 = 0.00103 from the area of the PSD. Figure 16 shows the sequence of 8000 data points simulated over 800 km for the -2 spectral slope and L_c= 1.75. When this result is compared with Figure 7, the increased filtering is evident. Again the simulated data retains the Gaussian PDF as shown in the histogram of Figure 17. The figure shows that the variance of the simulated data = 0.00102, matching the input parameter, σ^2. As shown in Figure 18, inputting a theoretical L_c= 10 and σ^2 = 0.0049 gives the predicted values of L_c= 9.98 from the PSD and 10 from the ACF, and σ^2 = 0.00491 from the area of the PSD. The values for the simulated curves are L_c= 9.37 from the PSD and 9.39 from the ACF, and σ^2 = 0.00472 from the area of the PSD. Figure 19 shows the sequence of 8000 data points simulated over 800 km for the -2 spectral slope and L_c= 10. Figure 20 again shows that the histogram of the simulated data retains the Gaussian PDF and that the variance of the simulated data = 0.00468, approximating the input parameter, σ^2.

Figure 21 repeats the calculations for a theoretical spectral slope of -3, L_c= 1.75, and σ^2 = 0.00102. Up to this point the autocorrelation function has been modified at zero lag as discussed above. However, as evident in Figure 21, for slopes of -2 and greater, the modified ACF results in a divergence of the predicted PSD at high wavenumbers whereas the unmodified ACF produces

good fidelity at high wavenumbers. For this reason, use of the modified ACF is appropriate only for the -5/3 spectral slope. For slopes of -2 and larger, subsequent analysis will use the unmodified ACF exclusively.

Figures 22-27 show the result of repeating the calculations for a spectral slope of -3. Figures 22-24 have inputted spectral parameters of L_c = 1.75 and σ^2 = 0.00102 while Figures 25-27 have L_c = 10 and σ^2 = 0.0049. For a slope of -3, using 6 coefficients for the predicted PSD and 12 coefficients for the simulated PSD, good agreement obtains between theoretical, predicted, and simulated curves, although there is less agreement at low wavenumbers for L_c = 10. For a theoretical L_c= 1.75, σ^2 = 0.00102, the predicted values are L_c= 1.88 from the PSD and 1.88 from the ACF, and σ^2 = 0.00102 from the area of the PSD. The values for the simulated curves are L_c= 1.79 from the PSD and 1.79 from the ACF, and σ^2 = 0.00102 from the area of the PSD. Figure 23 shows the sequence of 8000 data points simulated over 800 km for the -3 spectral slope and L_c= 1.75. Comparisons with Figure 16 show the -3 versus -2 increased filtering. Again the simulated data retains the Gaussian PDF as shown in the histogram of Figure 24. The figure shows that the variance of the simulated data = 0.00102, matching the input parameter, σ^2. As shown in Figure 25, inputting a theoretical L_c= 10 and σ^2 = 0.0049, gives predicted values of L_c= 16.6 from the PSD and 16.6 from the ACF, and σ^2 = 0.00490 from the area of the PSD. The values for the simulated curves are L_c= 16.1 from the PSD and 16.1 from the ACF, and σ^2 = 0.00473 from the area of the PSD. Figure 26 shows the sequence of 8000 data points simulated over 800 km for the -3 spectral slope and L_c= 10. Figure 27 again shows that the histogram of the simulated data retains the Gaussian PDF and that the variance of the simulated data = 0.00471, approximating the input parameter, σ^2. Figure 28 shows the improvement that is made by using 12 predictor coefficients. In this case, the predicted values are L_c= 13 from the PSD and 13 from the ACF, and σ^2 = 0.00490.

The final spectral slope examined in this report is for a slope = -4. Figures 29-34 present the results of repeating the calculations for a S = -4. Figures 29-31 have inputted spectral parameters of L_c = 1.75 and σ^2 = 0.00102 while Figures 32-34 have L_c = 10 and σ^2 = 0.0049. In this case, using 6 coefficients for the predicted PSD and 12 coefficients for the simulated PSD yields good agreement between theoretical, predicted, and simulated curves. For a theoretical L_c= 1.75, σ^2 = 0.00102, the predicted values are L_c= 1.75 from the PSD and 1.75 from the ACF, and σ^2 = 0.00102 from the area of the PSD. The values for the simulated curves are L_c= 1.67 from the PSD and 1.67 from the ACF, and σ^2 = 0.00102 from the area of the PSD. Figure 30 shows the sequence of 8000 data points simulated over 800 km for the -4 spectral slope and L_c= 1.75. Comparisons with Figure 23 show the -4 versus -3 increased filtering effect. Again the simulated data retains the Gaussian PDF as shown in the histogram of Figure 31. The figure shows that the variance of the simulated data = 0.00102, matching the input parameter, σ^2. As shown in Figure 32, inputting a theoretical L_c= 10 and σ^2 = 0.0049, gives predicted values of L_c= 9.98 from the PSD and 9.98 from the ACF, and σ^2 = 0.00490 from the area of the PSD. The values for the simulated curves are L_c= 10.1 from the PSD and 10.1 from the ACF, and σ^2 = 0.00463 from the area of the PSD. Figure 33 shows the sequence of 8000 data points simulated over 800 km for the -4 spectral slope and L_c= 10. Figure 34 again shows that the histogram of the simulated data

retains the Gaussian PDF and that the variance of the simulated data = 0.00461, approximating the input parameter, σ^2.

Up to this point the analysis has been based on a data spacing of 100 m. The effect of doubling the spacing is demonstrated in Figures 35 and 36. These plots have inputted spectral parameters of S = -5/3 and L_c = 5. Figure 35, which was calculated for a data spacing of 200 m, may be compared with Figure 36 which has a data spacing of 100 m. Of course, doubling the data spacing from 100 to 200 m halves the spatial resolution and reduces the Nyquist frequency from 5 km^{-1} to 2.5 km^{-1}. If reducing resolution is acceptable, the positive effect is the improvement in the predicted correlation length. For example, by using 6 linear predictor coefficients, the predicted L_c= 3.6 km for a spacing of 100 m but L_c= 4.28 km for a spacing of 200 m.

6. CONCLUSION

Geophysical phenomena within a specified domain often are characterized by smooth continuous power spectral densities having a negative power law slope. The association of one-, two-, and three-dimensional geophysical spectral densities with a given autocorrelation function was reviewed and the autoregressive methods of modern spectral estimation were explored. An autoregressive alternative to the more common Fourier transform analysis was studied with a goal of reducing the enormous computational burden of generating synthetic structure scenes from Gaussian random number sets. A 6 coefficient AR run to simulate 1300 points, using the Phillips Laboratory model 210 Convex computer, showed an average execution time of 0.462 ms, an improvement of a factor of 6.91/0.462 over the fast Fourier transform. In generating two-dimensional synthetic arrays, greater savings would result due to the 8-fold symmetry of the quarter-plane AR coefficients. It was demonstrated how the resolution and accuracy of predicted and simulated data, their PSD's and ACF's, and their parameters, change with spectral slope, correlation length, data spacing, and prediction order. In particular, six linear prediction coefficients are all that is necessary in many cases to generate a synthetic spatial sequence that retains a specified power law, correlation scale, variance, and probability distribution function. For a desired spectral slope of -5/3 one should employ an autocorrelation function having a modified zero lag value. For an equal linear predictor order, structured data having smaller correlation length, larger spectral slope, or reduced data resolution, have greater fidelity to specified characteristics than those generated for small slope, larger correlation length, or higher resolution. However, fidelity often can be reestablished by increasing the spectral order from 6 coefficients to 12 or in the worst case 20 coefficients. Since the maximum vertical correlation length over relevant SHARC altitudes is reported to be approximately 10 km, a vertical resolution of 100 m can be achieved with a minimum of coefficients. However, since maximum horizontal correlation lengths are reported to be approximately 85 km, horizontal resolution must be sacrificed or else many more coefficients must be used to achieve fidelity at both low and high frequencies. Where low frequency simulation is unimportant, one may retreat to a minimum number of coefficients and still achieve fidelity at mid and high frequencies.

Autoregressive (AR) and autoregressive moving average (ARMA) modeling should be considered in creating large atmospheric structured scenes. A subsequent report will address the potential for using two-dimensional ARMA modeling to generate two and three-dimensional structured scenes.

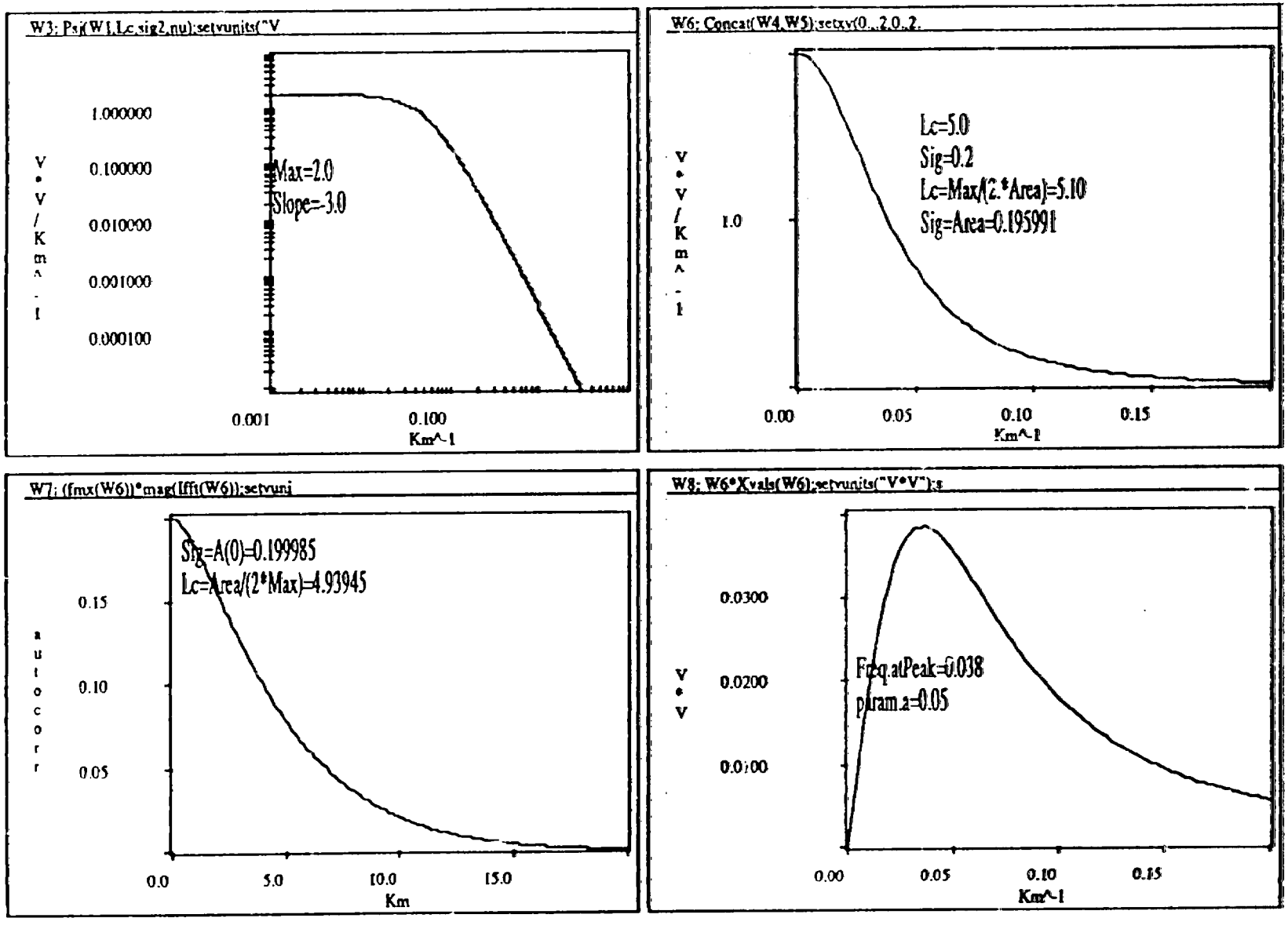

Figure 1. Sample model PSD and autocorrelation function, Slope = 3., $\sigma^2 = 0.2$, $L_c = 5.0$ and a = 0.05. Upper left quadrant log-log PSD vs spatial frequency, upper right quadrant linear PSD plot, lower left quadrant autocorrelation function vs lag, lower right quadrant, power curve

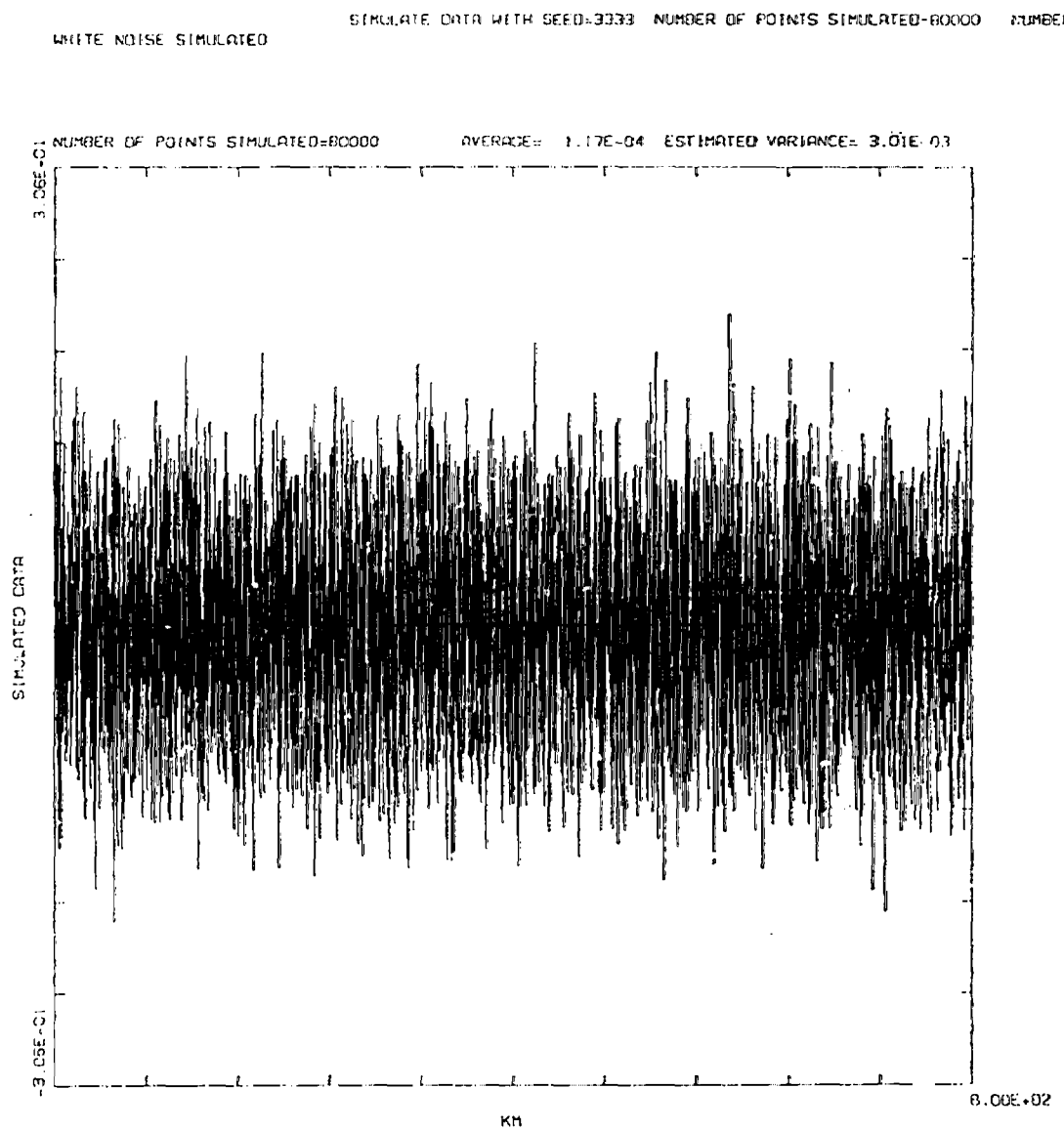

Figure 2. White noise. Sample Gaussian random number sequence, mean = 0., standard deviation = 0.055, spacing 100 m

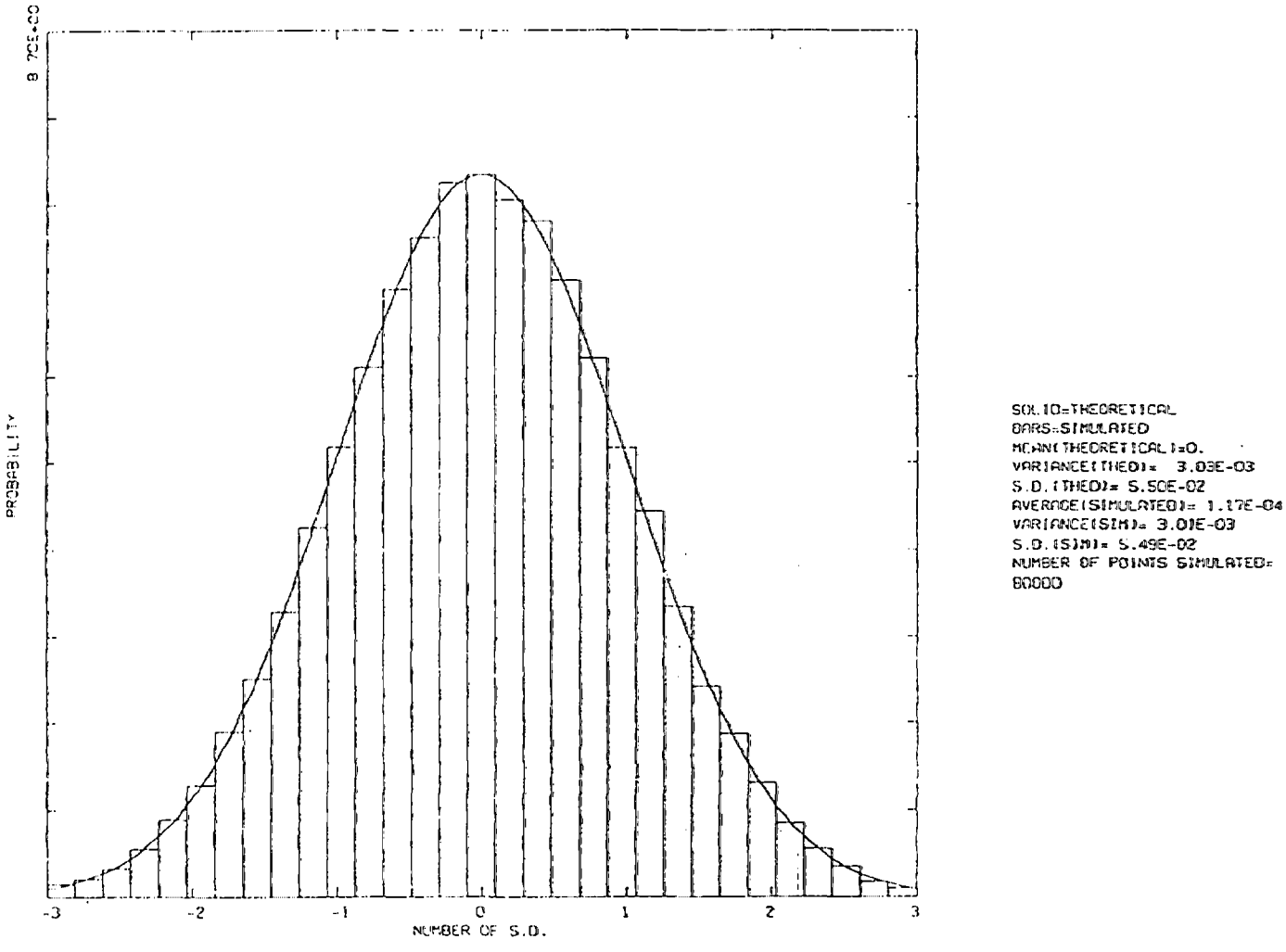

Figure 3. Histogram of sample Gaussian random number sequence. Theoretical mean = 0., theoretical S.D. = 0.055.

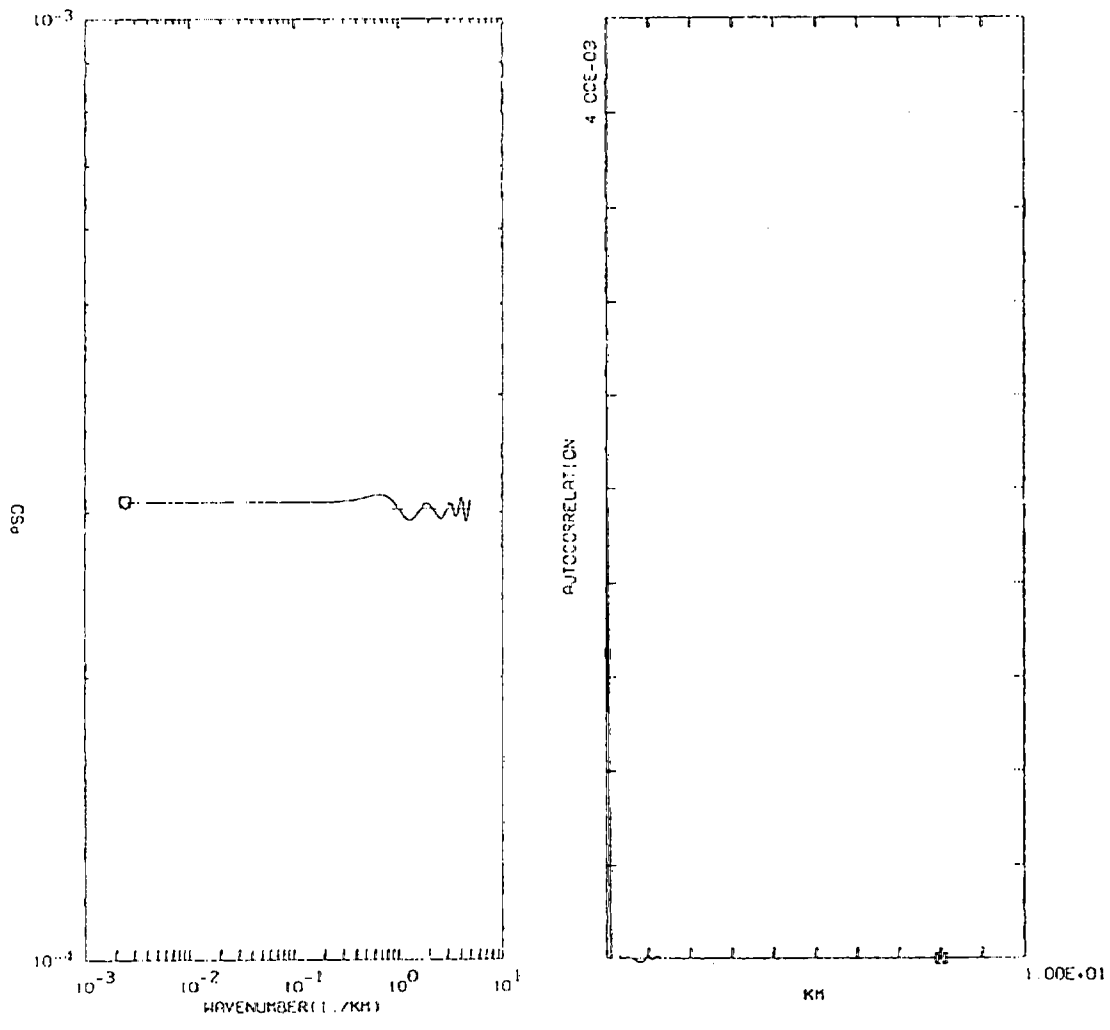

Figure 4. White noise power spectral density of raw Gaussian random number sequence, mean = 0., S.D. = 0.055

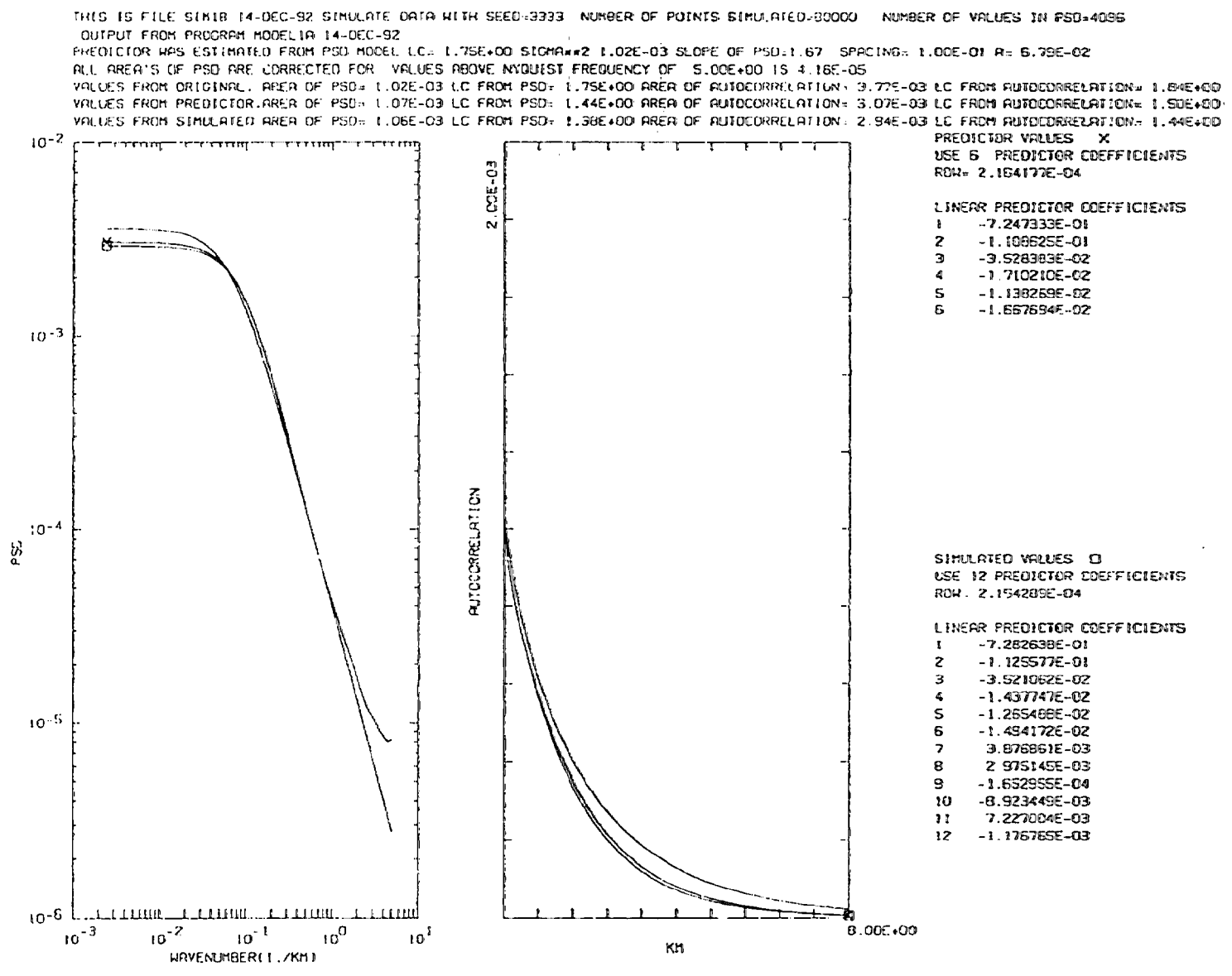

Figure 5. Left panel, theoretical PSD input (unmarked), autoregressive predictor PSD (marked by x), and simulated PSD (marked by small square). Right panel, corresponding autocorrelation functions. L_c = 1.75 km, log-log spectral slope = -5/3 , σ^2 = 1.02E-03, spacing = 100 m. Unmodified theoretical autocorrelation function. Six predictor coefficients.

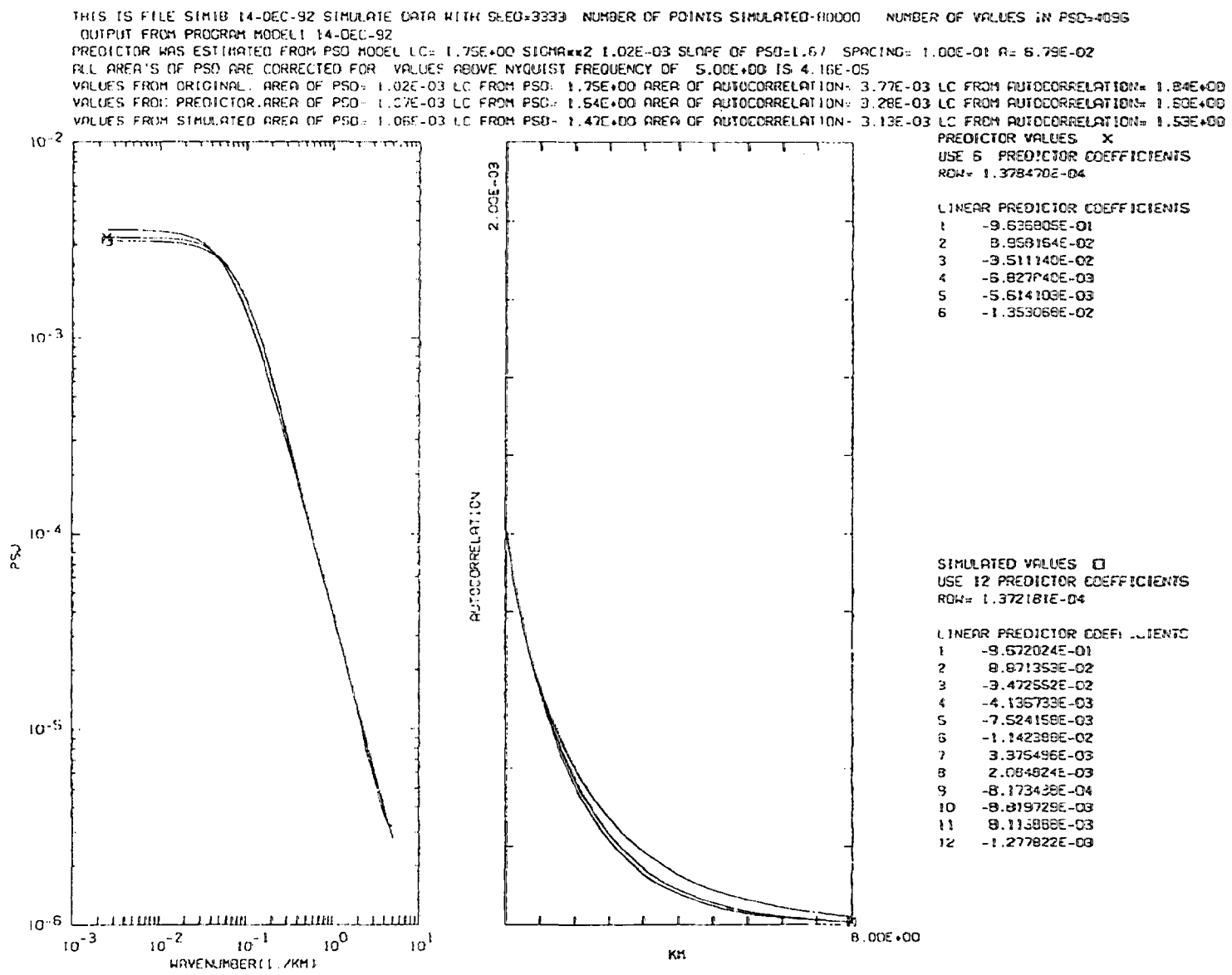

Figure 6. Left panel, theoretical PSD input (unmarked), autoregressive predictor PSD (marked by x), and simulated PSD (marked by small square). Right panel, corresponding autocorrelation functions. L_c = 1.75 km, S = -5/3, σ^2 = 1.02E-03, spacing = 100 m. Theoretical autocorrelation function modified at lag = 0. Six predictor coefficients

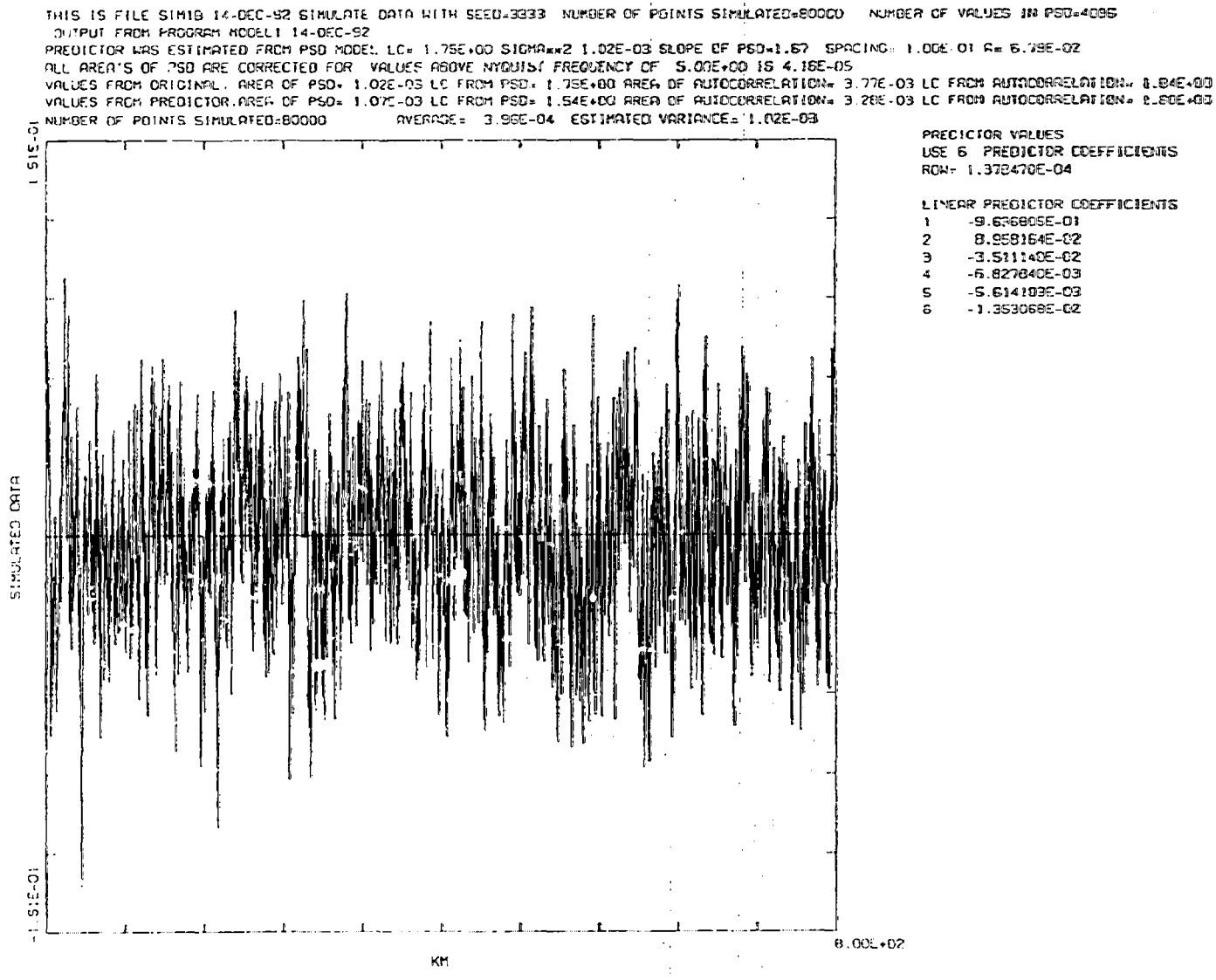

Figure 7. Autoregressive simulated structure sequence. L_c = 1.75 km, S = -5/3, σ^2 = 1.02E-03

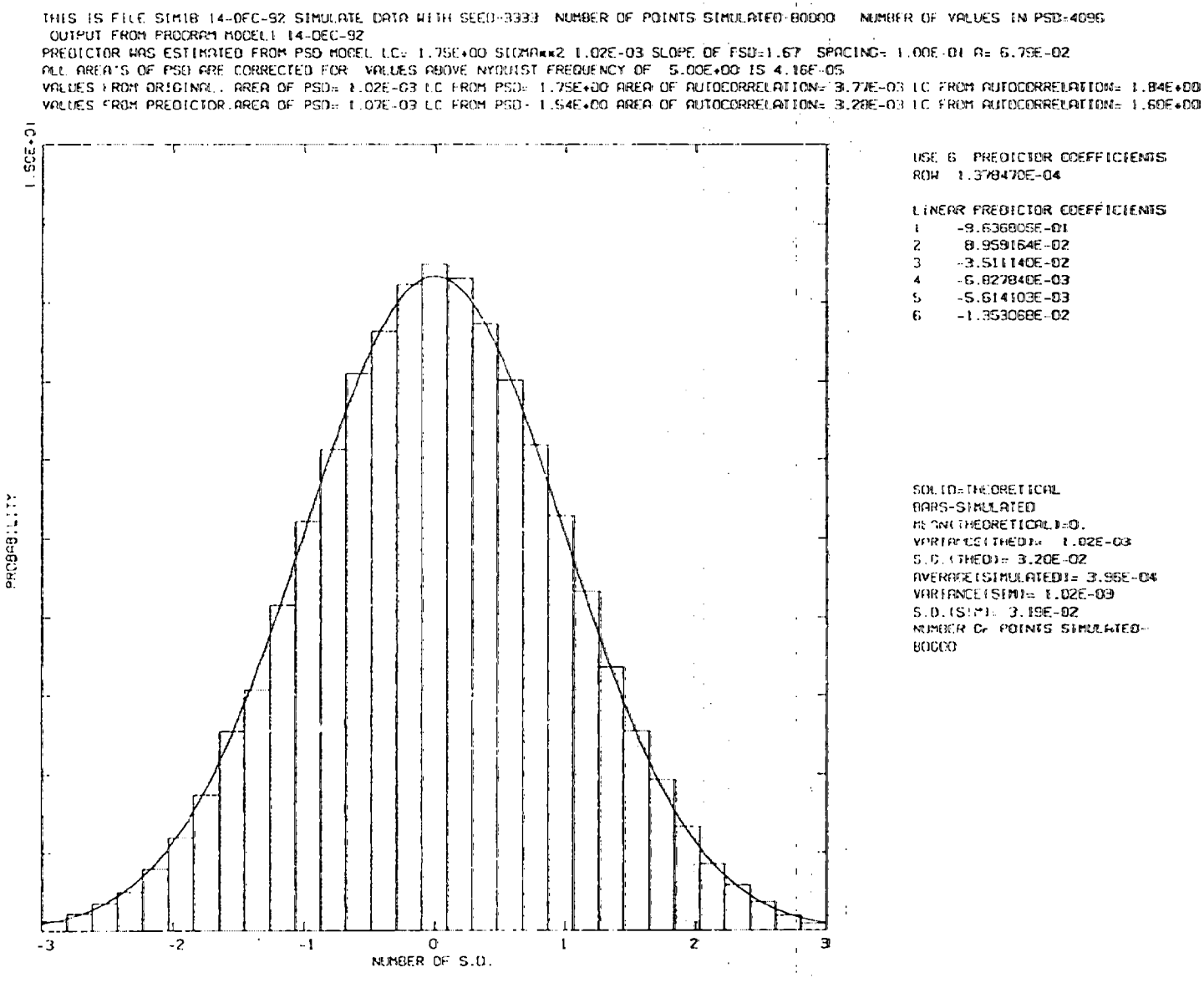

Figure 8. Histogram of autoregressive simulated structure sequence. L_c = 1.75 km, S = -5/3, σ^2 = 1.02E-03

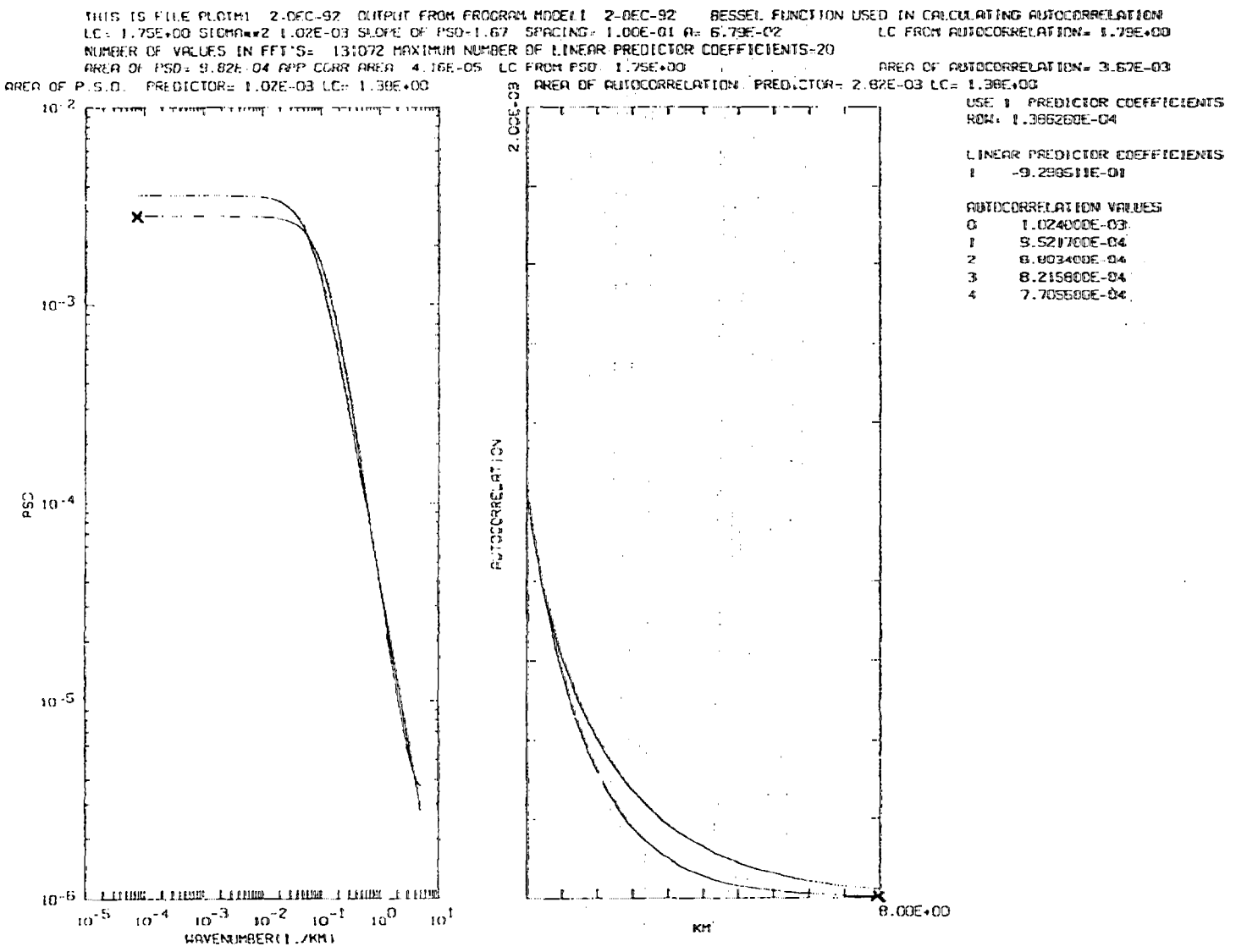

Figure 9. Left panel, theoretical PSD input (unmarked), autoregressive predictor PSD (marked by x). Right panel, corresponding autocorrelation functions. L_c = 1.75 km, S = -5/3 σ^2 = 1.02E-03, spacing = 100 m. Modified theoretical autocorrelation function at lag = 0. One predictor coefficient

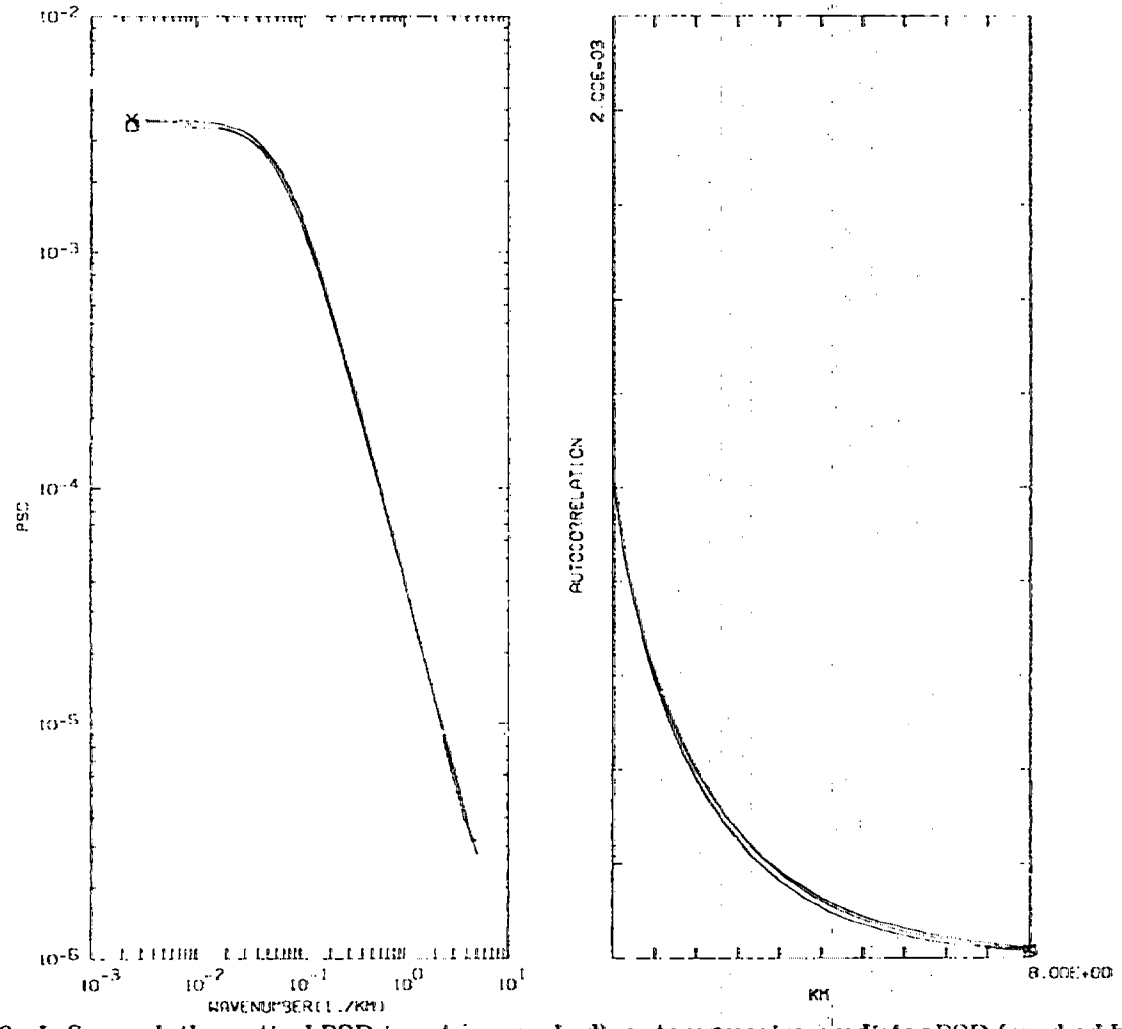

Figure 10. Left panel, theoretical PSD input (unmarked), autoregressive predictor PSD (marked by x), and simulated PSD (marked by small square). Right panel, corresponding autocorrelation functions. L_c = 1.75 km, S = -5/3, σ^2 = 1.02E-03, spacing = 100 m. Theoretical autocorrelation function modified at lag = 0. Twenty predictor coefficients

LC= 1.75E+00 SIGMA**2 1.02E-03 SLOPE OF PSD=1.67 SPACING= 1.00E-01 A= 6.79E-02 LC FROM AUTOCORRELATION= 1.79E+00
NUMBER OF VALUES IN FFT'S= 131072 MAXIMUM NUMBER OF LINEAR PREDICTOR COEFFICIENTS=20
AREA OF PSD= 9.82E-04 APP CORR AREA= 4.16E-05 LC FROM PSD= 1.75E+00 AREA OF AUTOCORRELATION= 3.67E-03

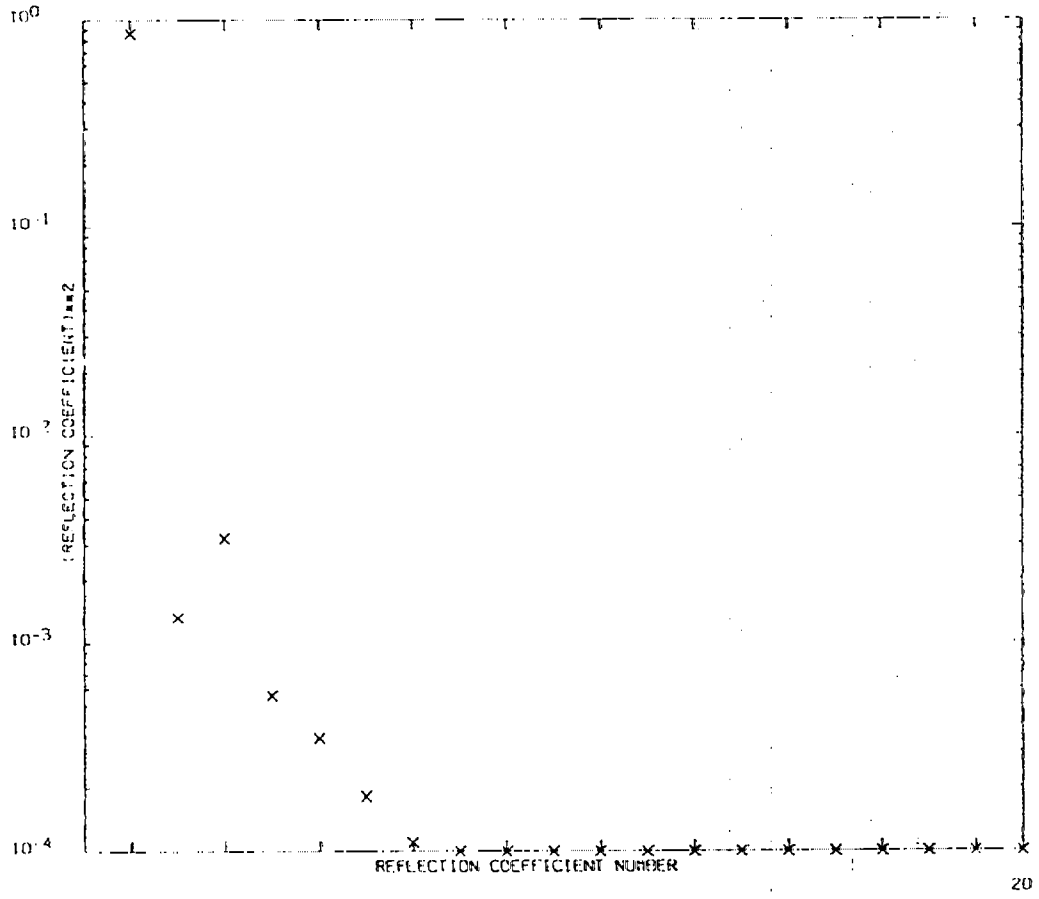

REFLECTION COEFFICIENT	
1	-9.298511E-01
2	3.634933E-02
3	-5.673431E-02
4	-2.360887E-02
5	-1.865677E-02
6	-1.353068E-02
7	-1.048312E-02
8	-8.302839E-03
9	-6.723633E-03
10	-5.535307E-03
11	-4.619264E-03
12	-3.898243E-03
13	-3.320988E-03
14	-2.852148E-03
15	-2.466669E-03
16	-2.146359E-03
17	-1.877736E-03
18	-1.650622E-03
19	-1.457219E-03
20	-1.291459E-03

Figure 11. Plot of the square of the reflection coefficient versus reflection coefficient number for twenty reflection coefficients. L_c = 1.75 km, S = -5/3, σ^2 = 1.02E-03, spacing = 100 m. Theoretical autocorrelation function modified at lag = 0

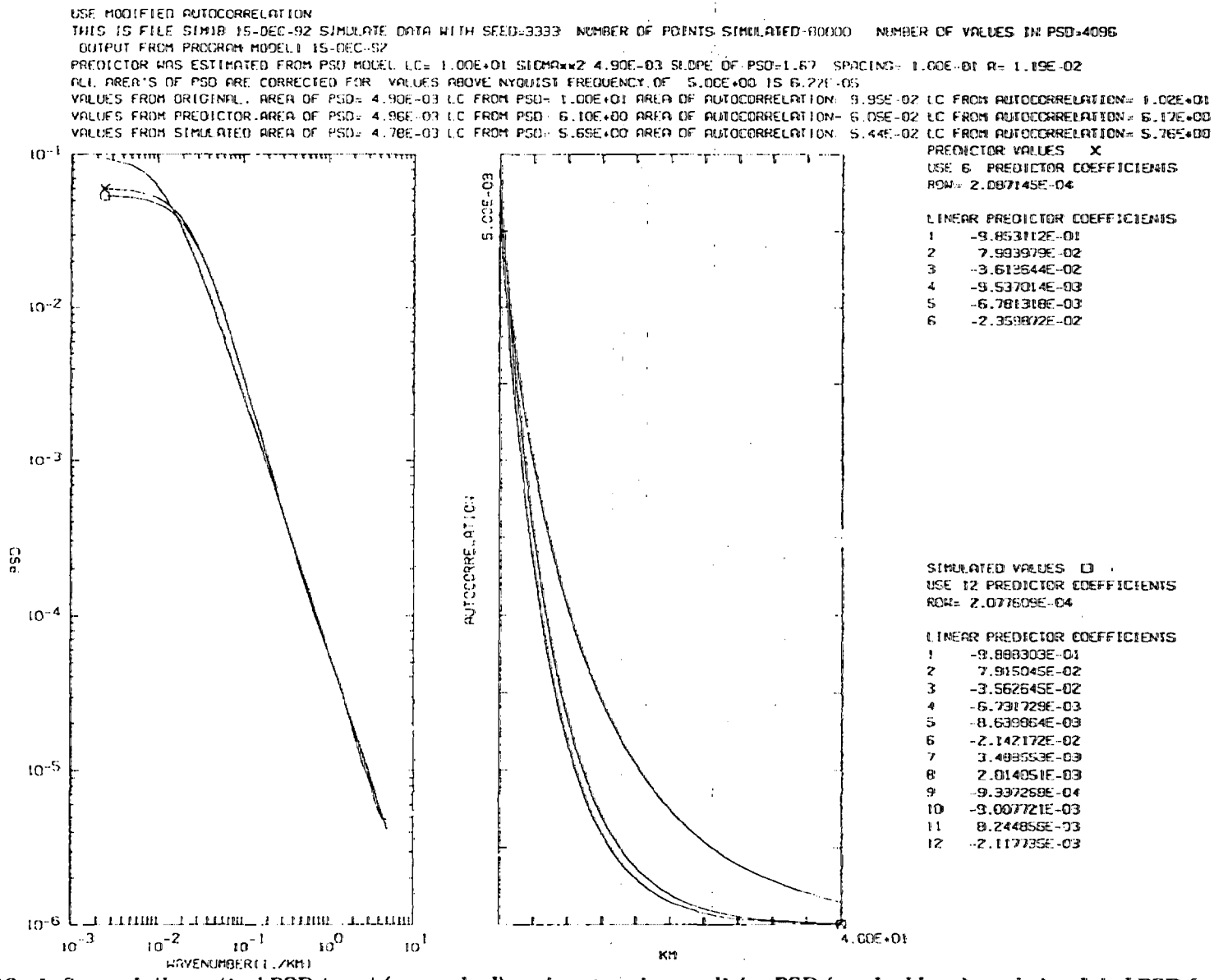

Figure 12. Left panel, theoretical PSD input (unmarked), autoregressive predictor PSD (marked by x), and simulated PSD (marked by small square). Right panel, corresponding autocorrelation functions. L_c = 10 km, S = -5/3, σ^2 = 4.9E-03, spacing = 100 m. Theoretical autocorrelation function modified at lag = 0. Six predictor coefficients

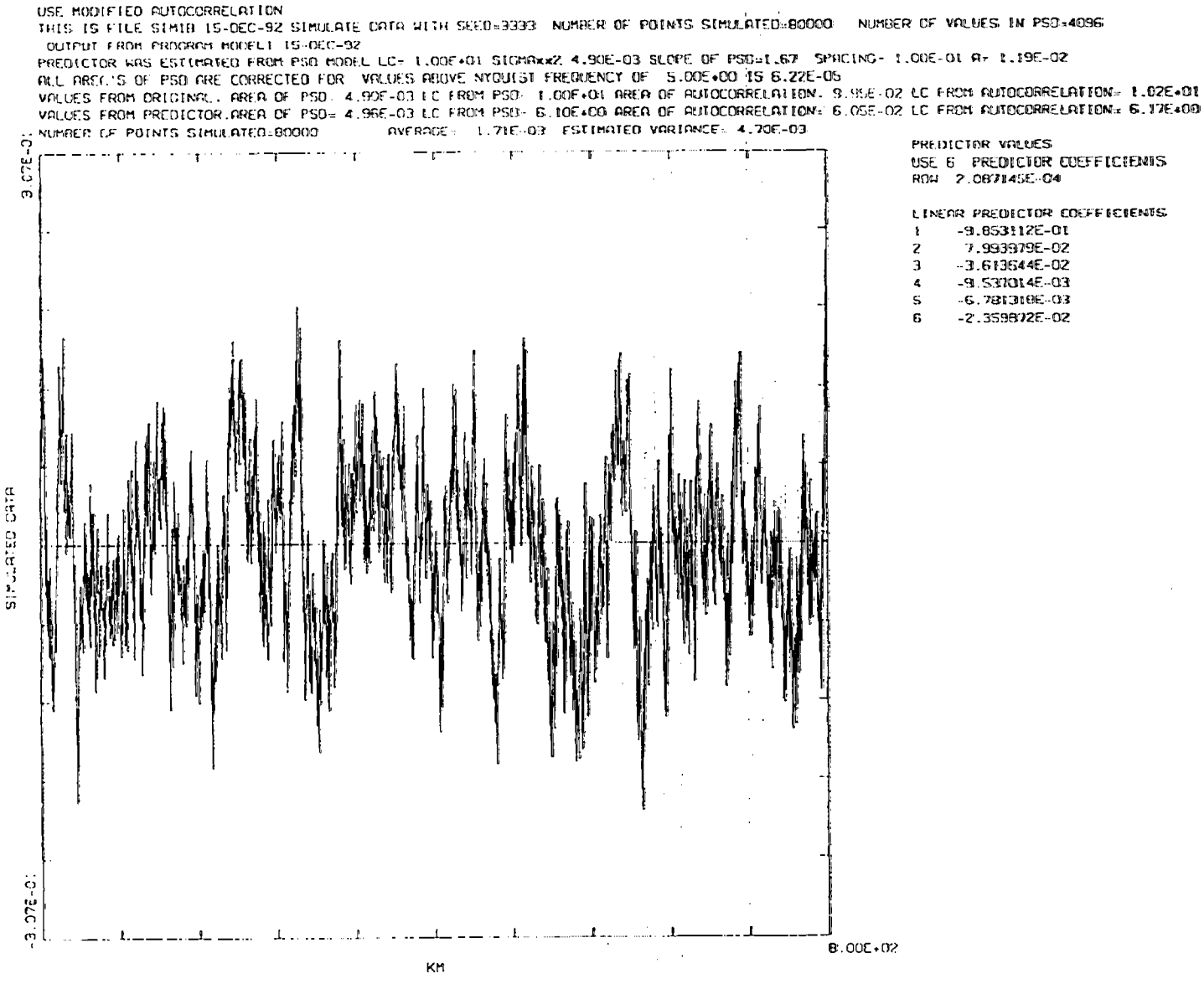

Figure 13. Autoregressive simulated structure sequence. L_c = 10 km, S = -5/3, σ^2 = 4.9E-03

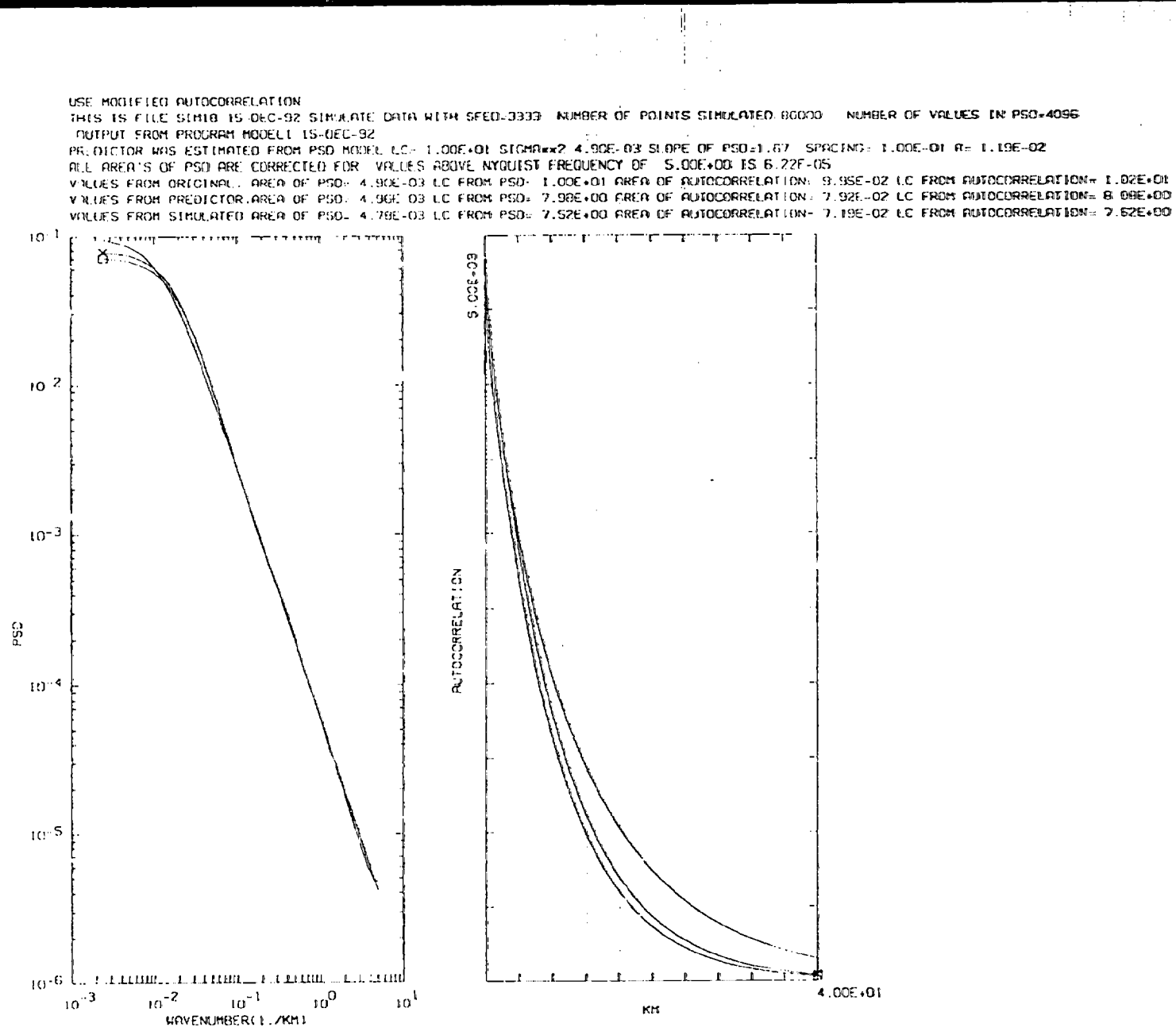

Figure 14. Left panel, theoretical PSD input (unmarked), autoregressive predictor PSD (marked by x), and simulated PSD (marked by small square). Right panel, corresponding autocorrelation functions. L_c = 10 km, S = -5/3, σ^2 = 4.9E-03, spacing = 100 m. Theoretical autocorrelation function modified at lag = 0. Twenty predictor coefficients

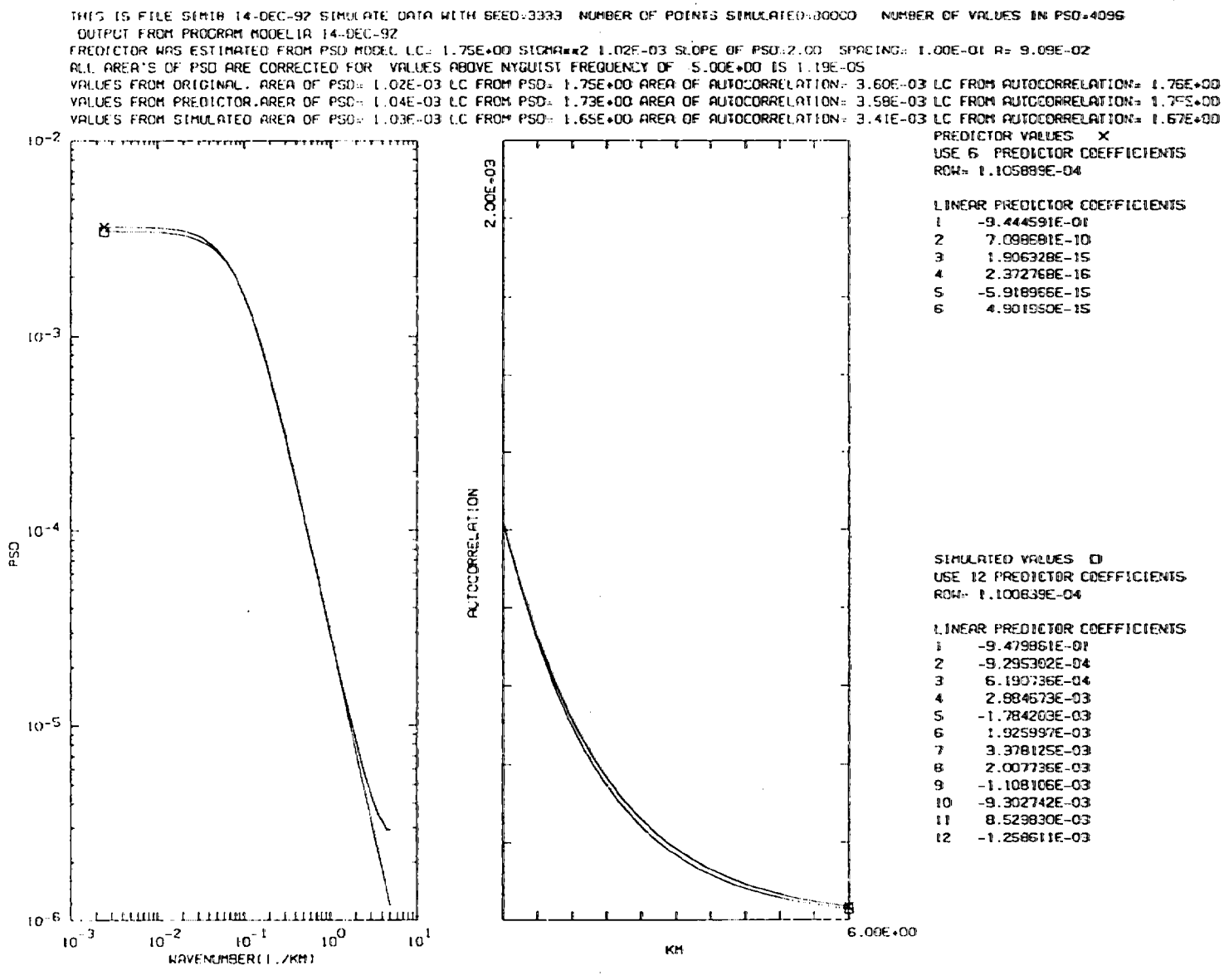

Figure 15. Left panel, theoretical PSD input (unmarked), autoregressive predictor PSD (marked by x), and simulated PSD (marked by small square). Right panel, corresponding autocorrelation functions. L_c = 1.75 km, S = -2, σ^2 = 1.02E-03, spacing = 100 m. Theoretical autocorrelation function modified at lag = 0. Six predictor coefficients

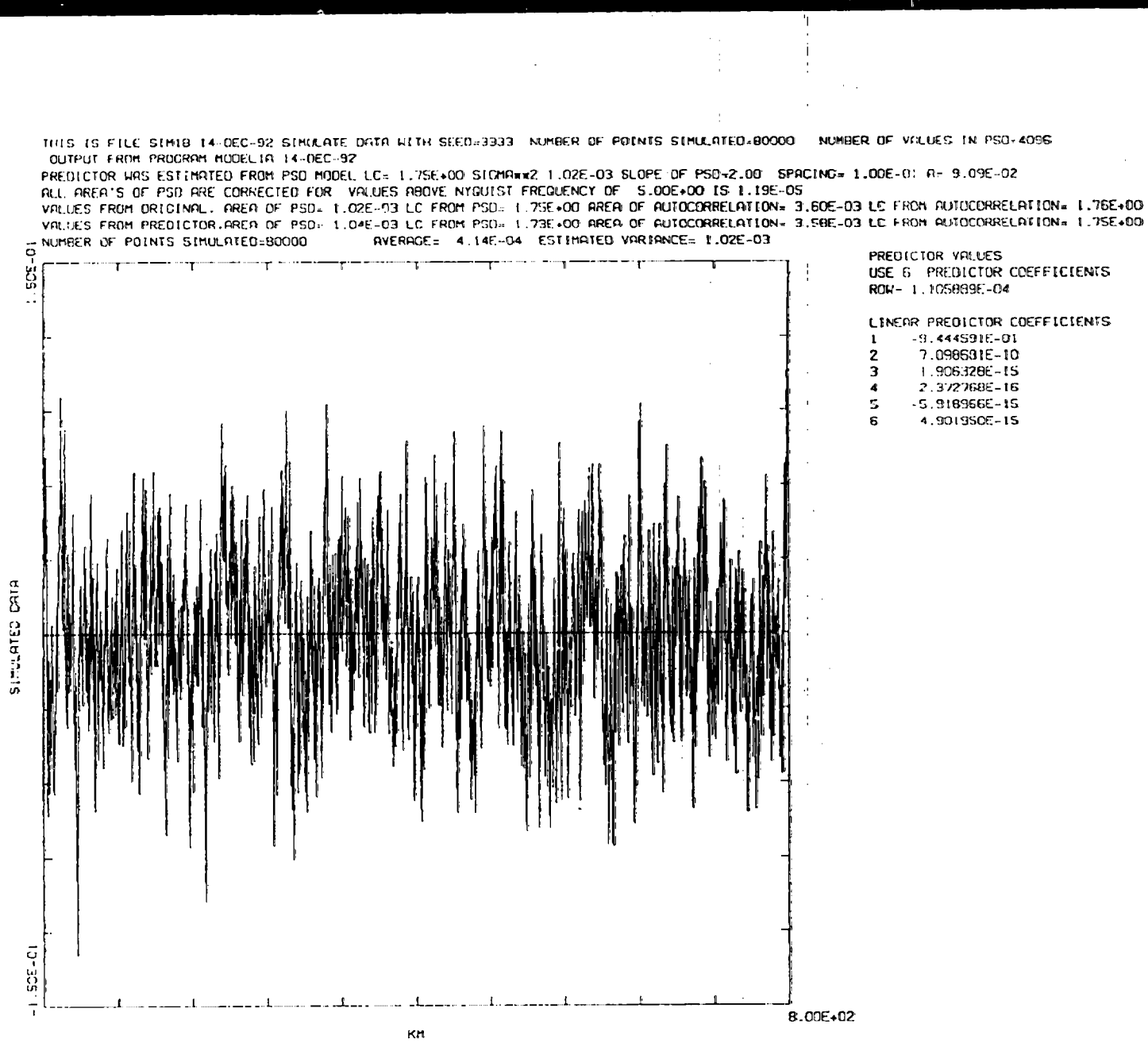

Figure 16. Autoregressive simulated structure sequence. L_c = 1.75 km, S = -2, σ^2 = 1.02E-03

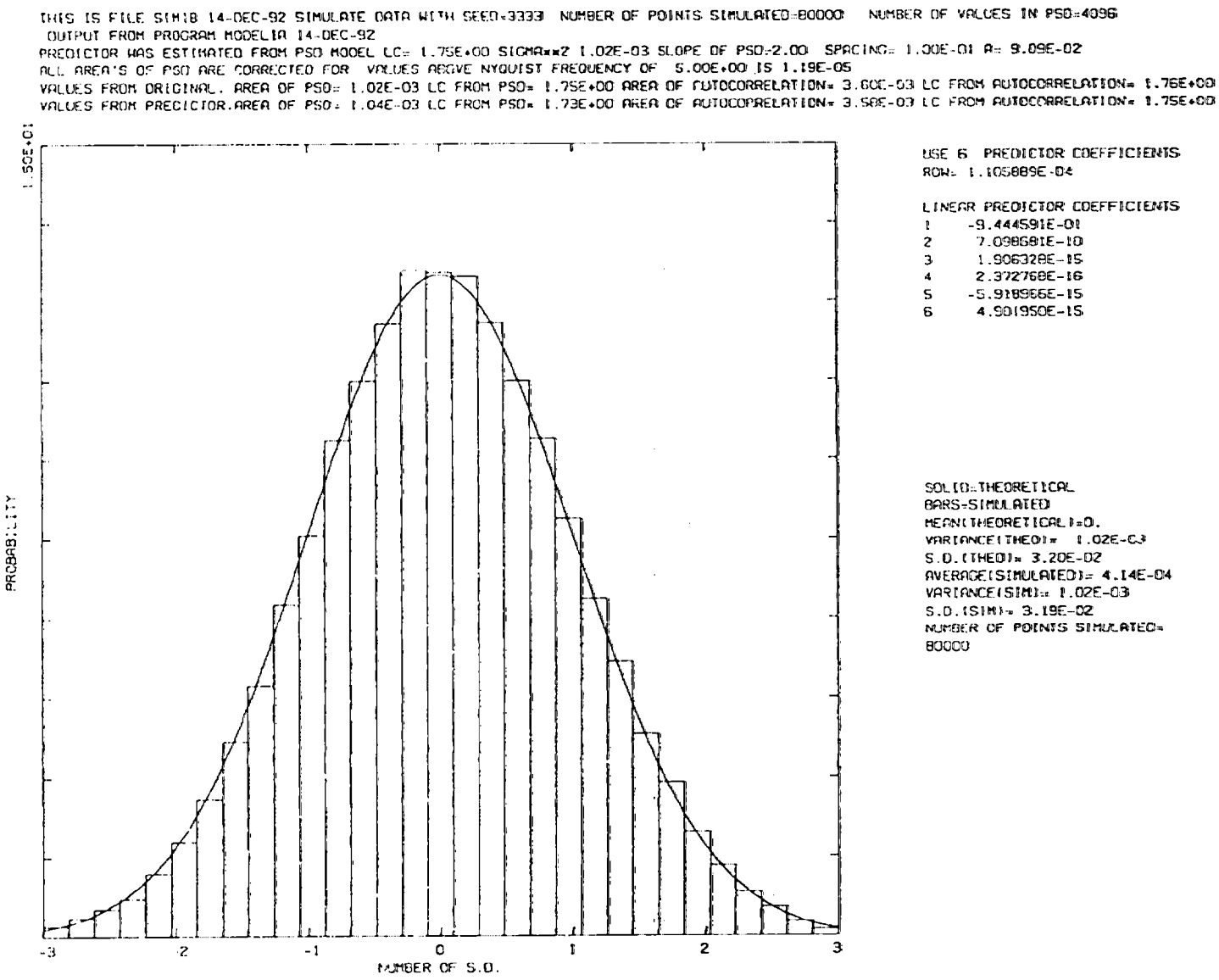

Figure 17. Histogram of autoregressive simulated structure sequence. L_c = 1.75 km, S = -2, σ^2 = 1.02E-03

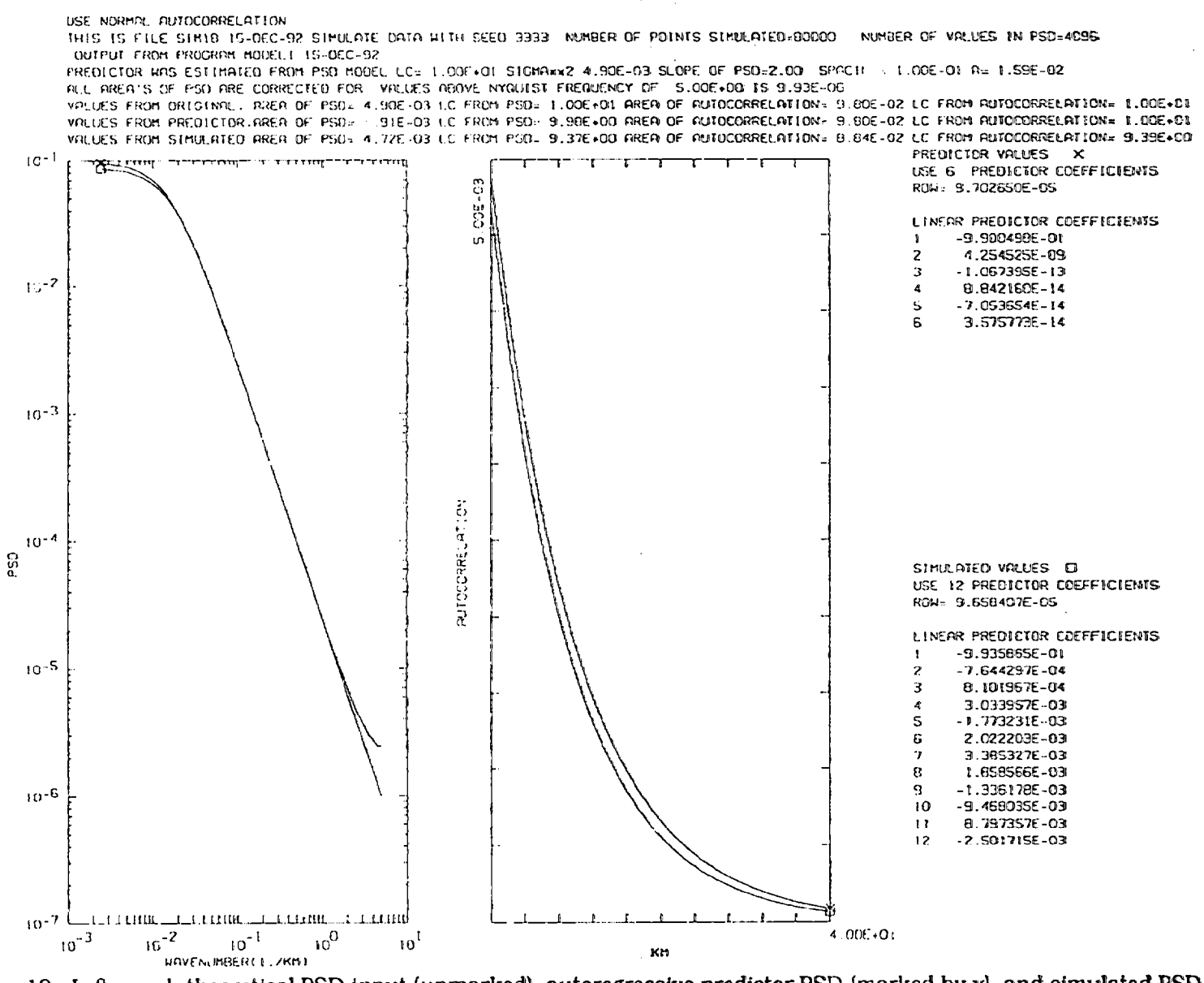

Figure 18. Left panel, theoretical PSD input (unmarked), autoregressive predictor PSD (marked by x), and simulated PSD (marked by small square). Right panel, corresponding autocorrelation functions. L_c = 10 km, S = -2, σ^2 = 4.9E-03, spacing = 100 m. Unmodified theoretical autocorrelation function. Six predictor coefficients

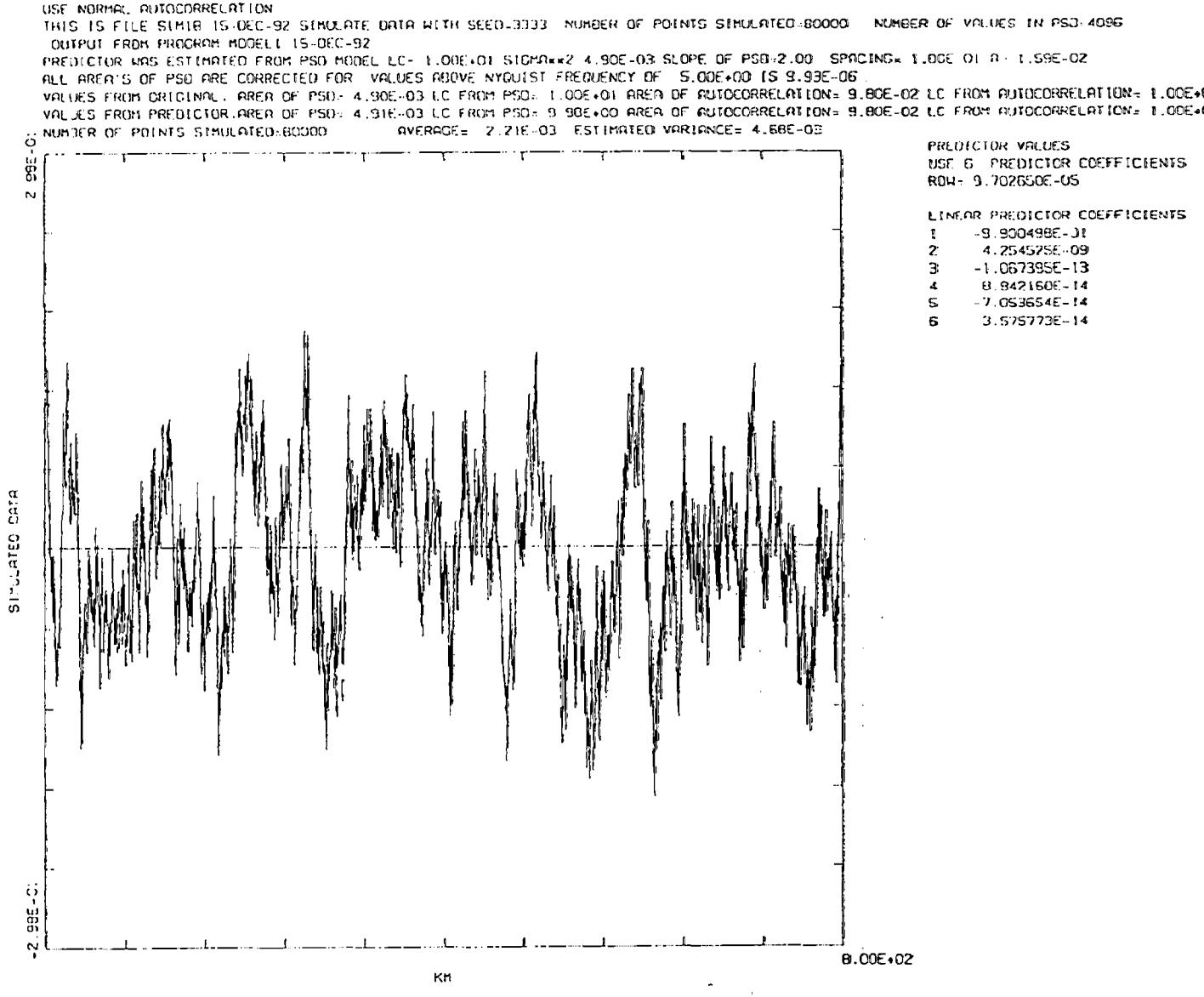

Figure 19. Autoregressive simulated structure sequence. L_c = 10 km, S = -2, σ^2 = 4.9E-03

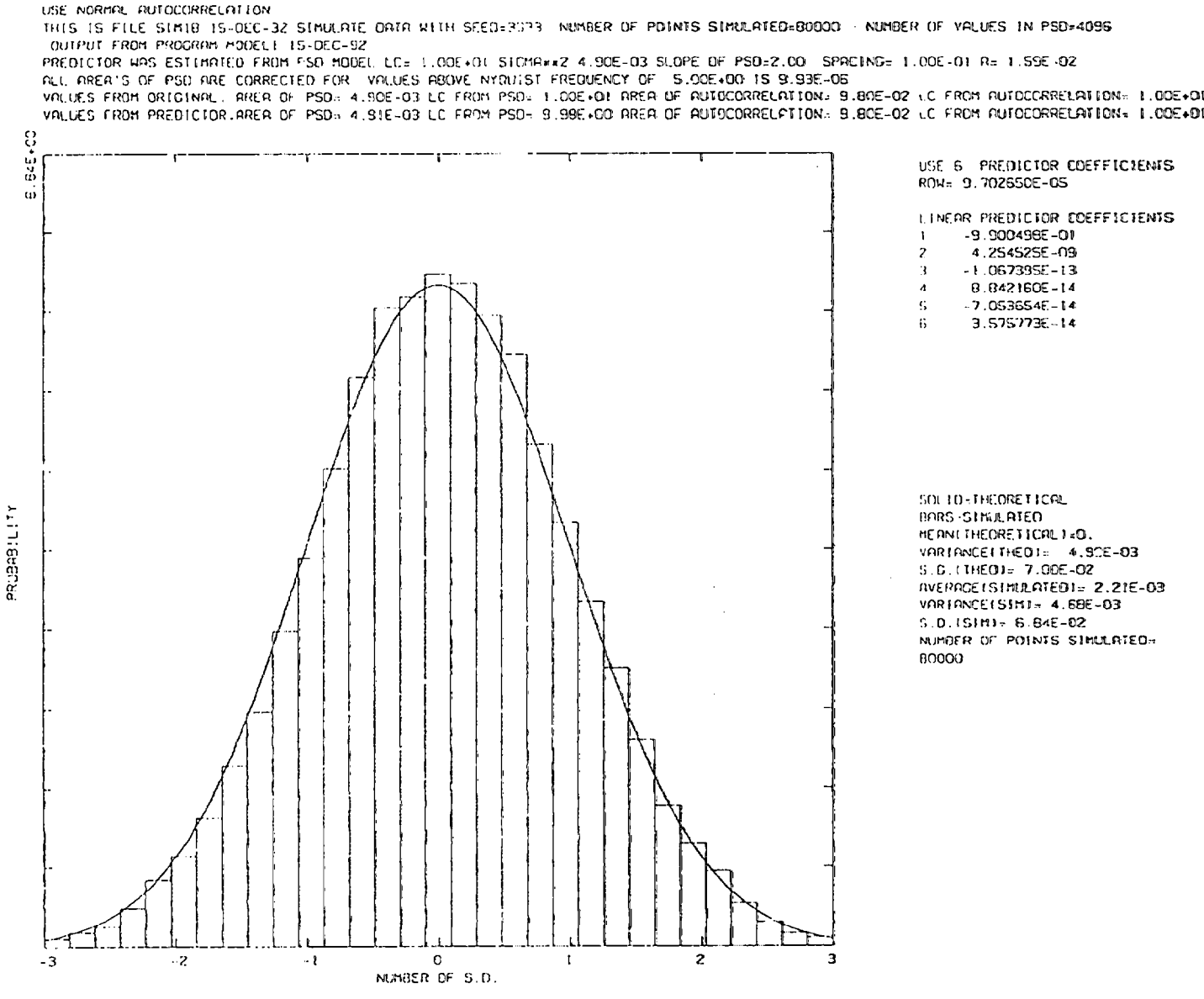

Figure 20. Histogram of autoregressive simulated structure sequence. L_c = 10 km, S = -2, σ^2 = 4.9E-03

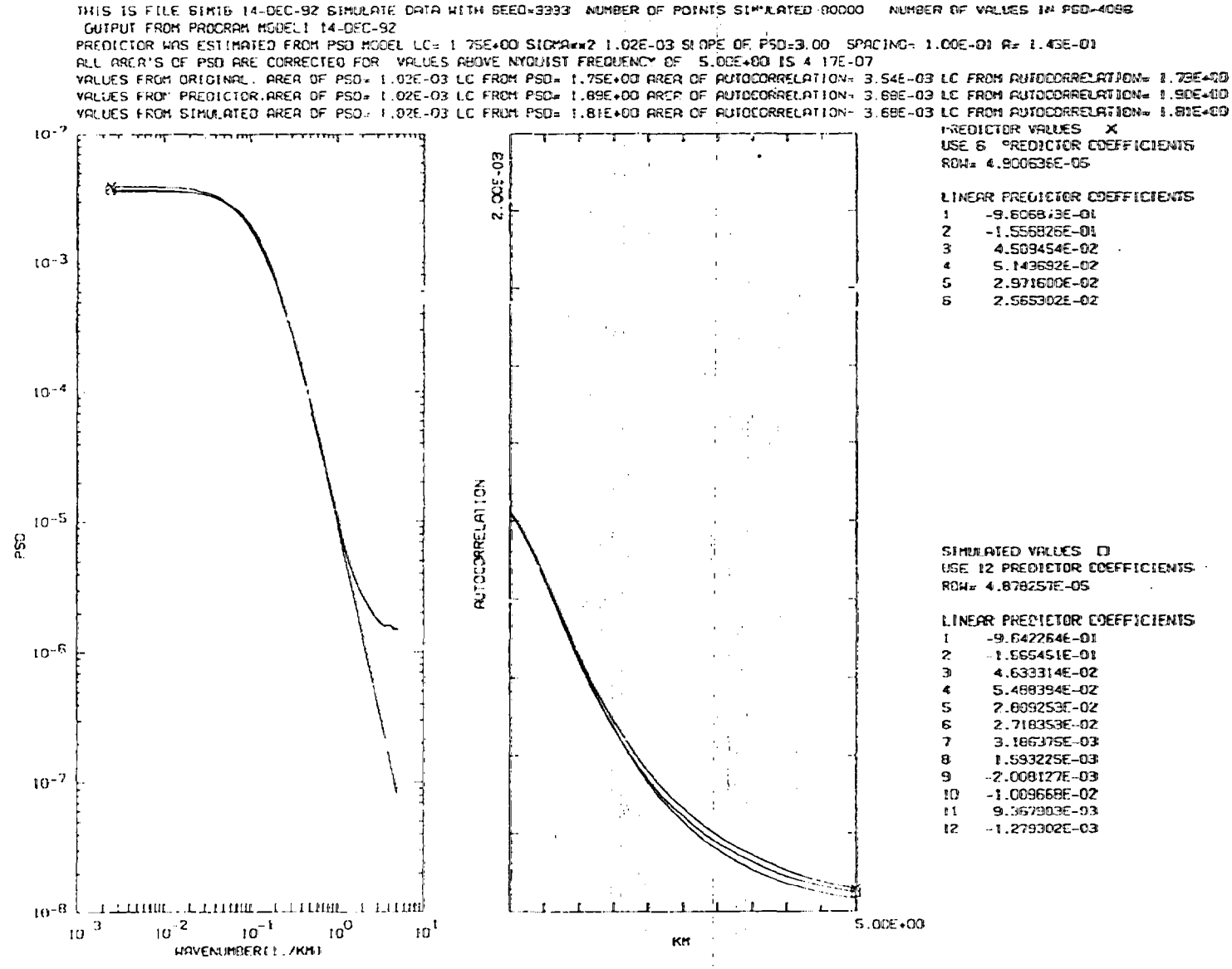

Figure 21. Left panel, theoretical PSD input (unmarked), autoregressive predictor PSD (marked by x), and simulated PSD (marked by small square). Right panel, corresponding autocorrelation functions. L_c = 1.75 km, S = -3, σ^2 = 1.02E-03, spacing = 100 m. Theoretical autocorrelation function modified at lag = 0. Six predictor coefficients

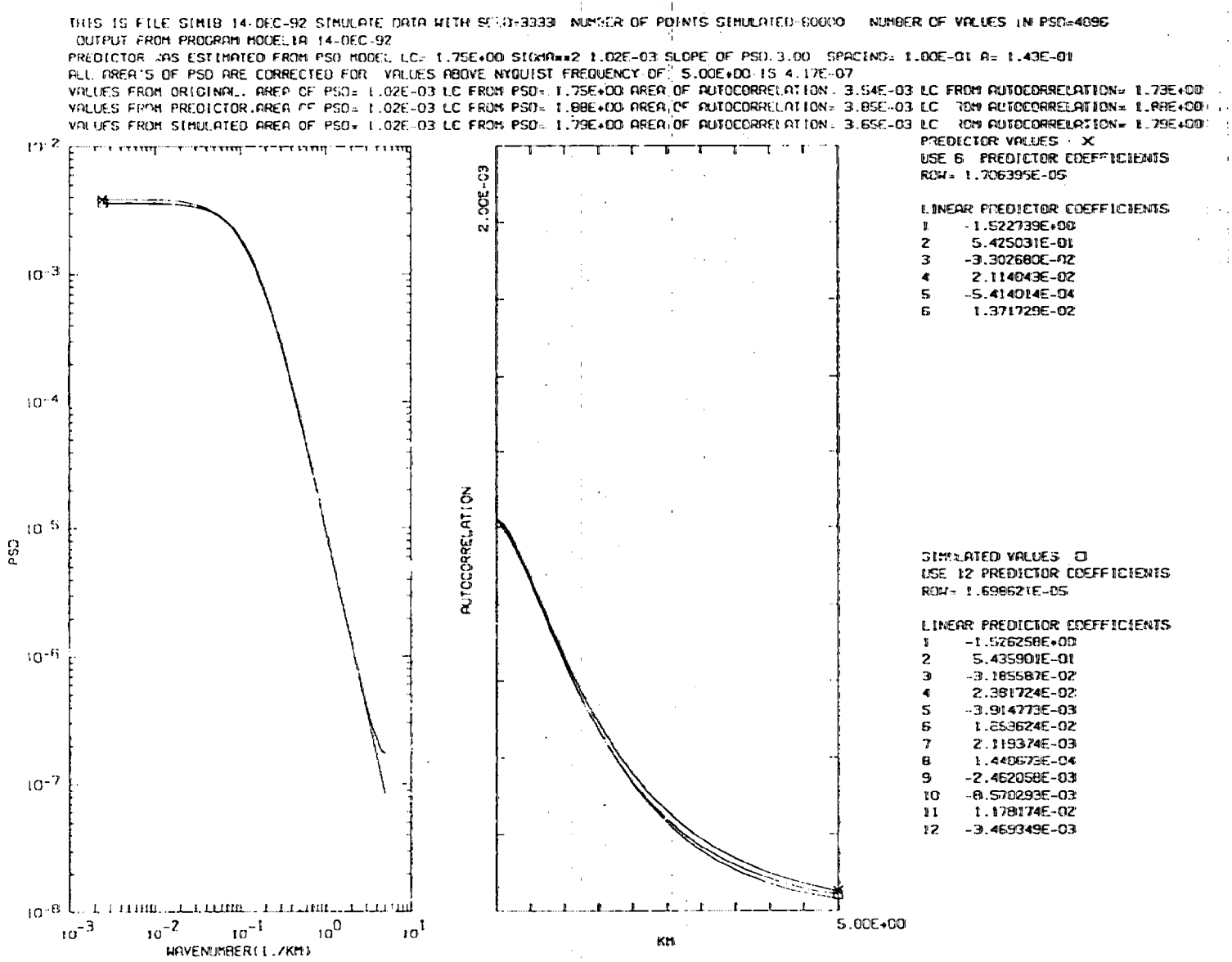

Figure 22. Left panel, theoretical PSD input (unmarked), autoregressive predictor PSD (marked by x), and simulated PSD (marked by small square). Right panel, corresponding autocorrelation functions. L_c = 1.75 km, S = -3, σ^2 = 1.02E-03, spacing = 100 m. Unmodified theoretical autocorrelation function. Six predictor coefficients

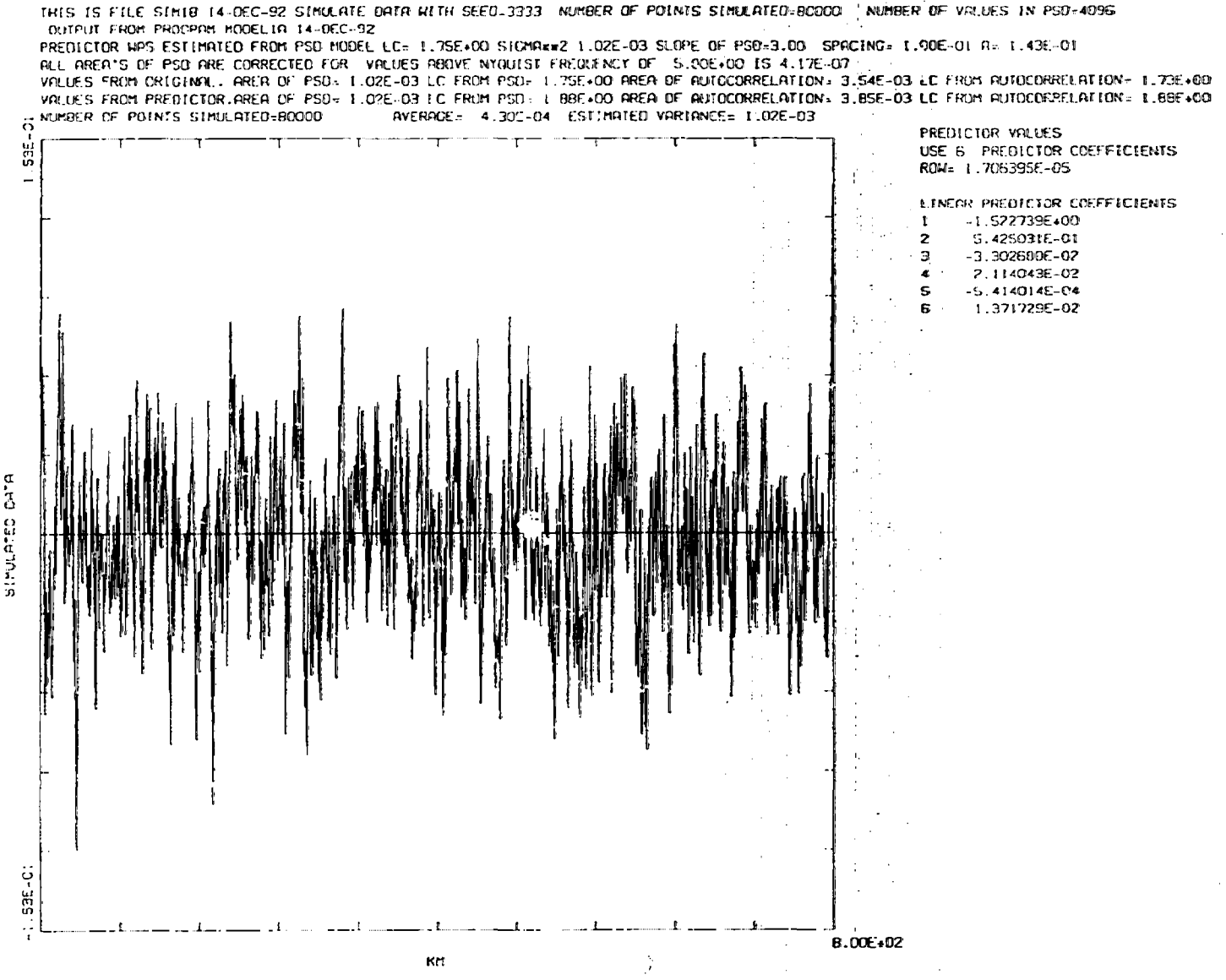

Figure 23. Autoregressive simulated structure sequence. L_c = 1.75 km, S = -3, σ^2 = 1.02E-03

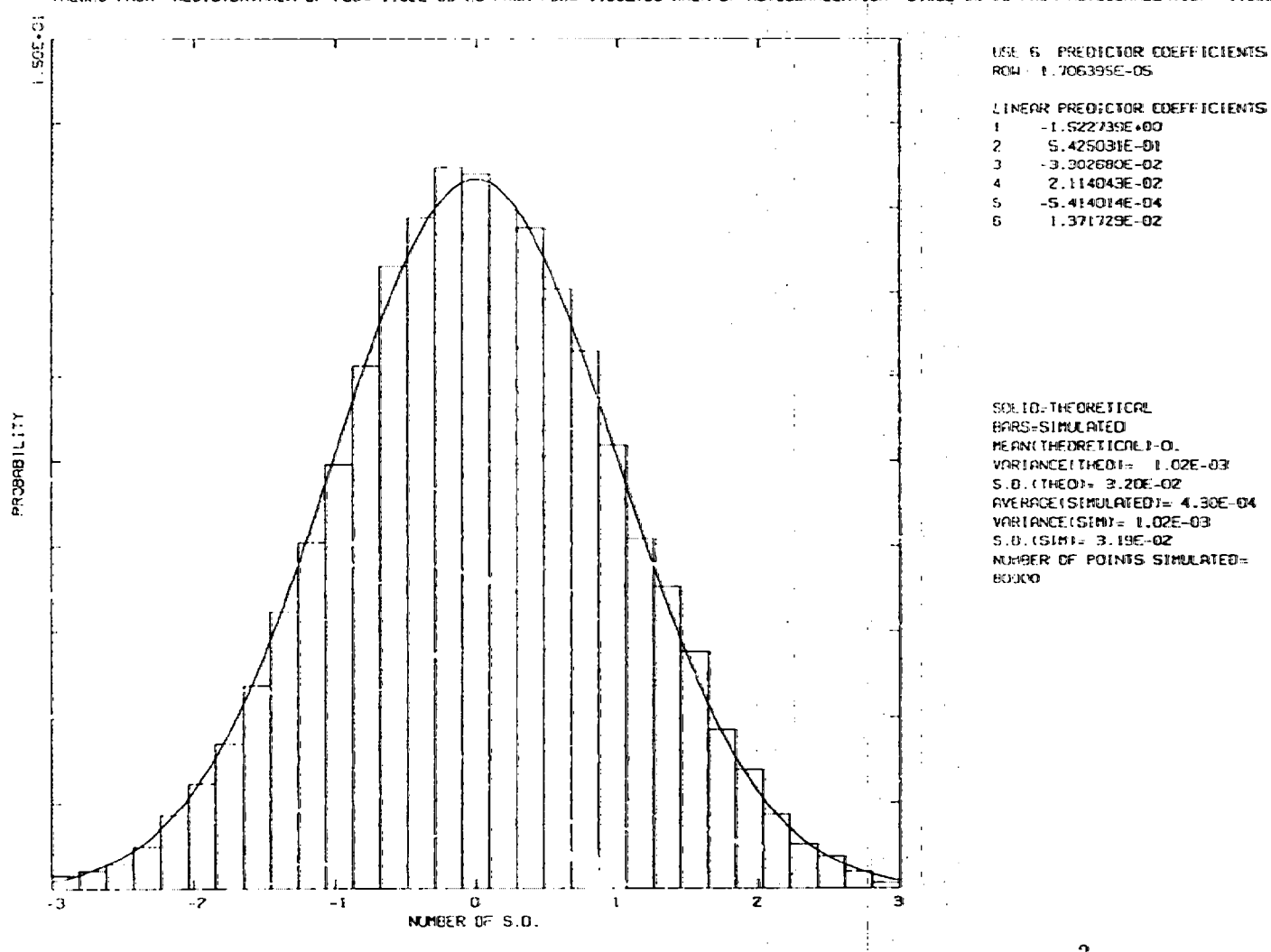

Figure 24. Histogram of autoregressive simulated structure sequence. L_c = 1.75 km, S = -3, σ^2 = 1.02E-03

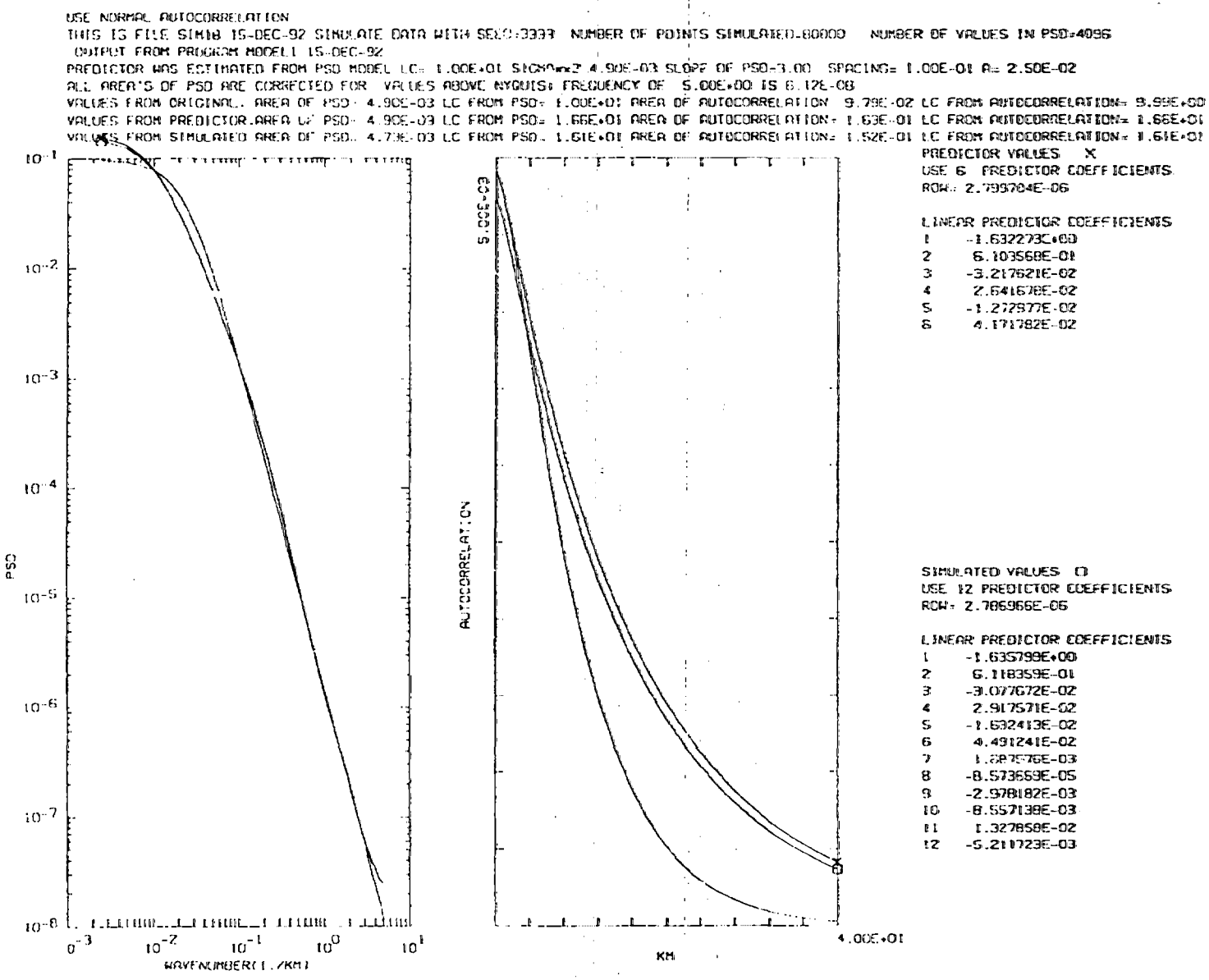

Figure 25. Left panel, theoretical PSD input (unmarked), autoregressive predictor PSD (marked by x), and simulated PSD (marked by small square). Right panel, corresponding autocorrelation functions. L_c = 10 km, S = -3, σ^2 = 4.9E-03, spacing = 100 m. Unmodified theoretical autocorrelation function. Six predictor coefficients

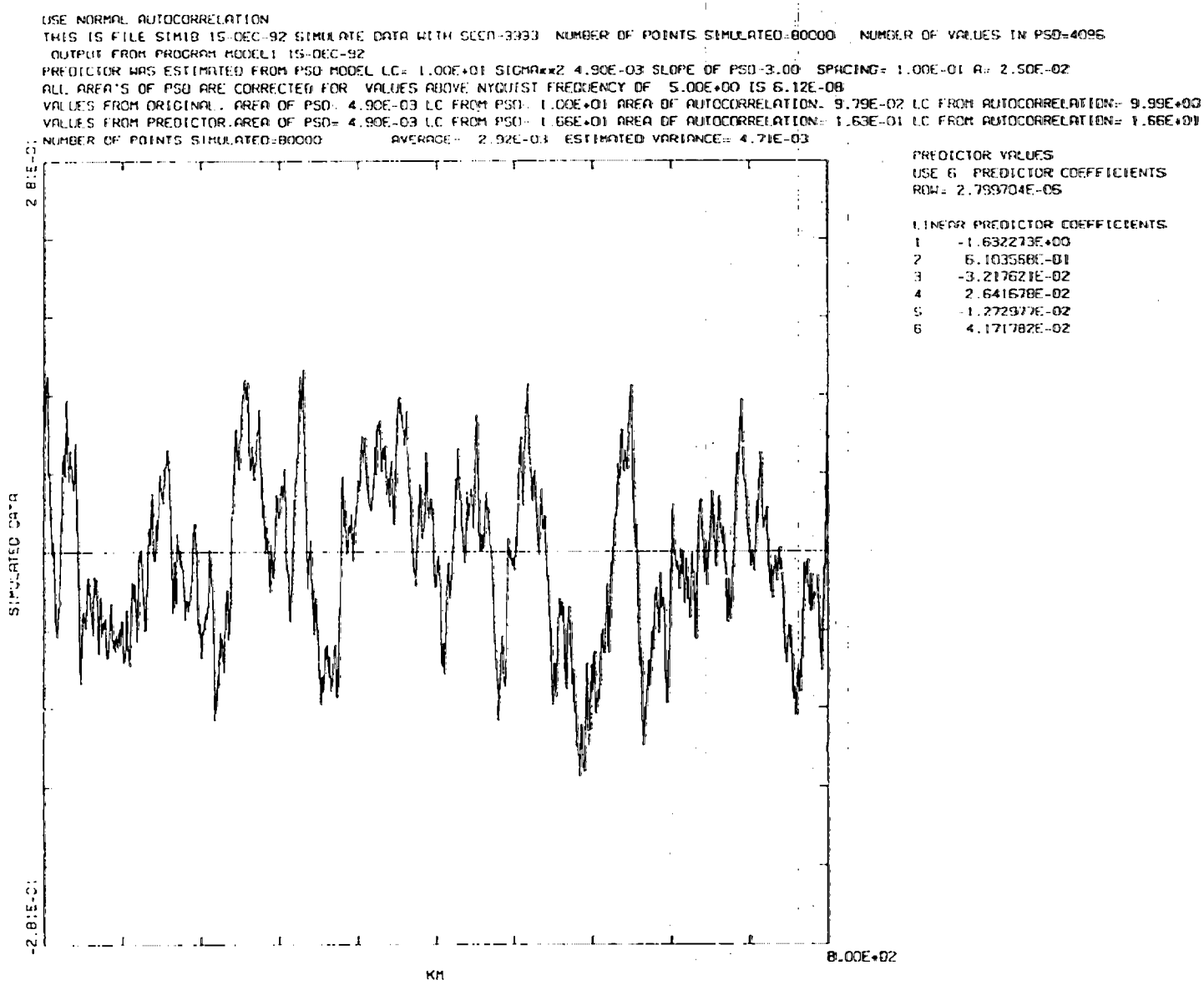

Figure 26. Autoregressive simulated structure sequence. L_c = 10 km, S = -3, σ^2 = 4.9E-03

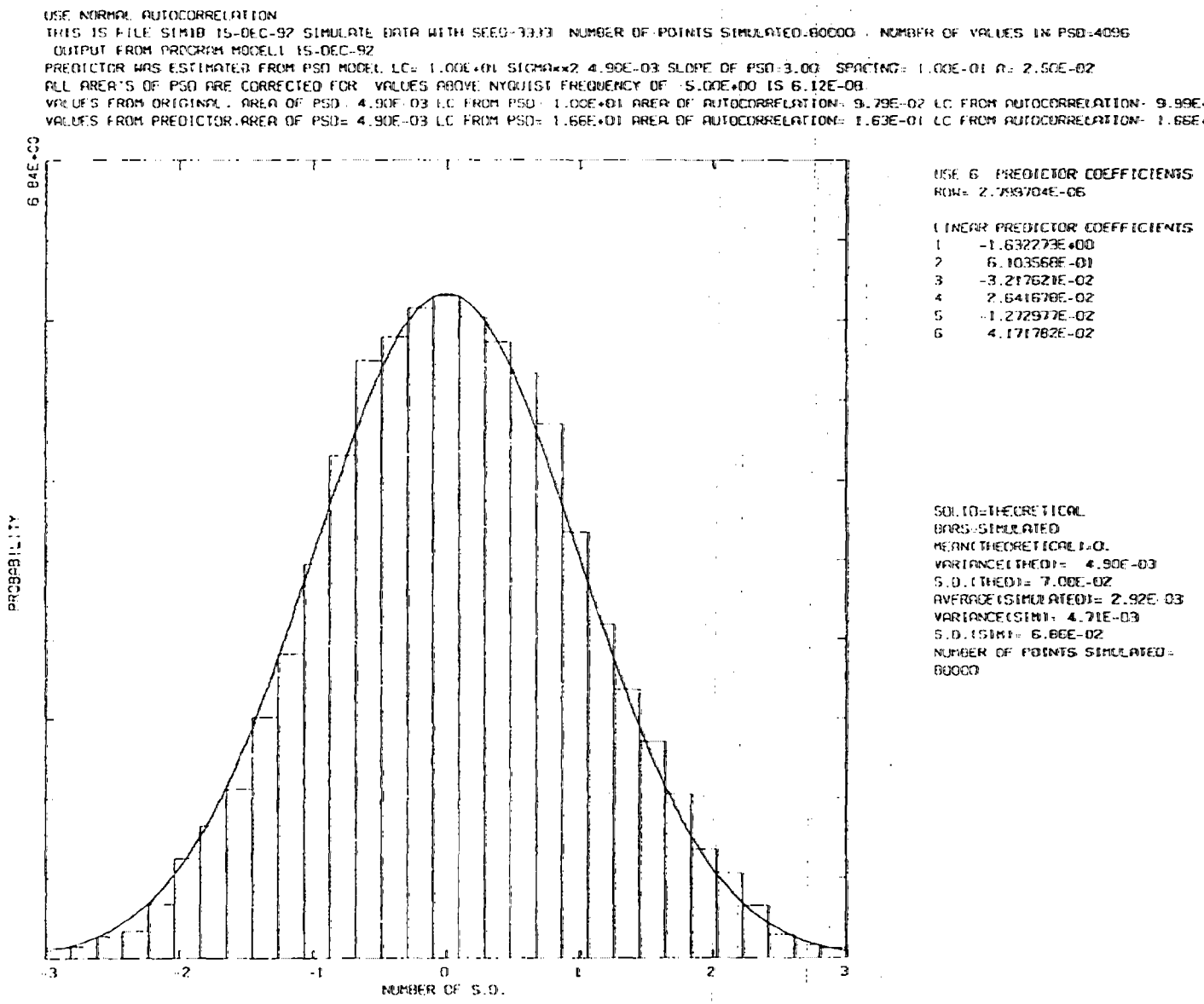

Figure 27. Histogram of autoregressive simulated structure sequence. L_c = 10 km, S = -3, σ^2 = 4.9E-03

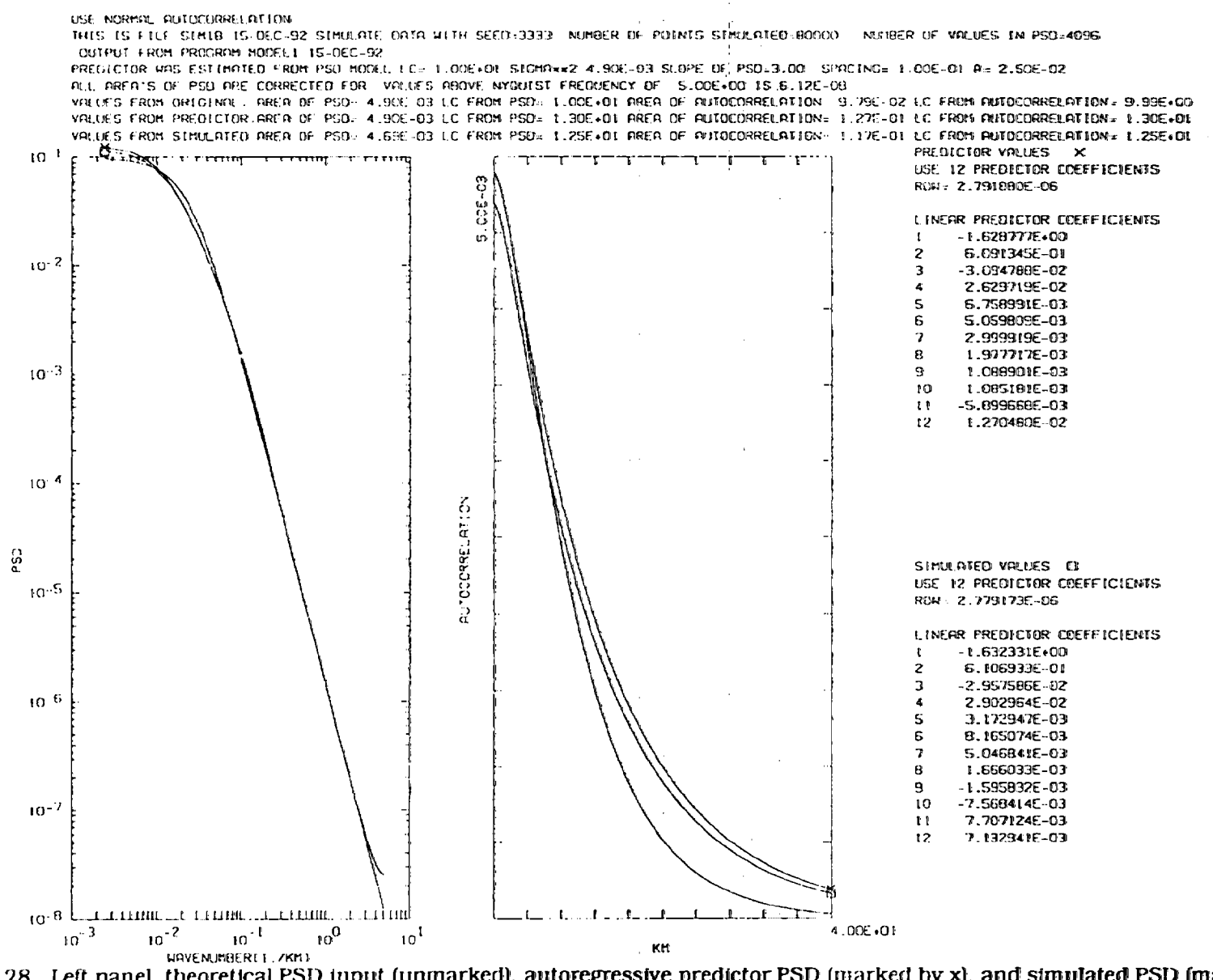

Figure 28. Left panel, theoretical PSD input (unmarked), autoregressive predictor PSD (marked by x), and simulated PSD (marked by small square). Right panel, corresponding autocorrelation functions. L_c = 10 km, S = -3, σ^2 = 4.9E-03, spacing = 100 m. Unmodified theoretical autocorrelation function. Twelve predictor coefficients

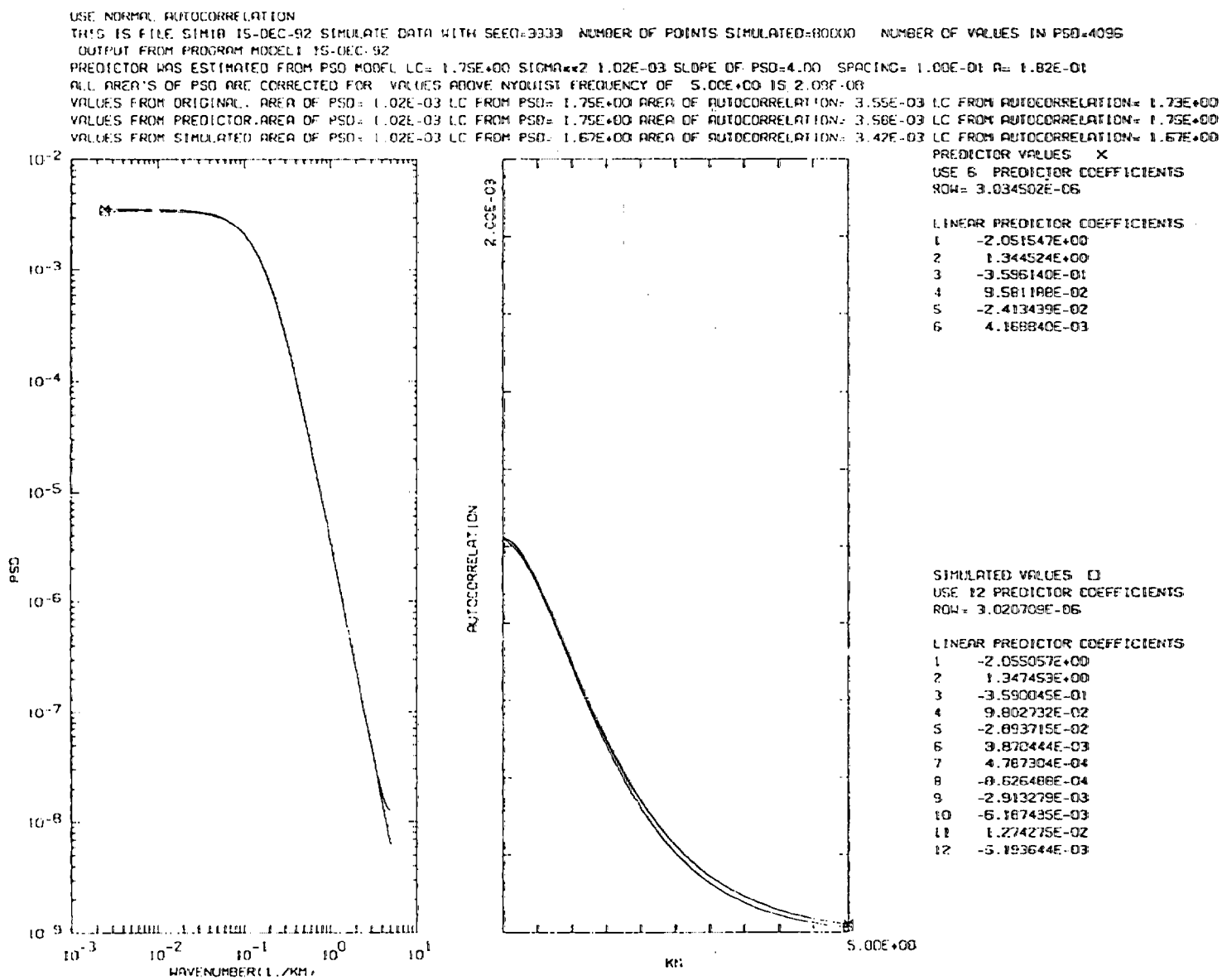

Figure 29. Left panel, theoretical PSD input (unmarked), autoregressive predictor PSD (marked by x), and simulated PSD (marked by small square). Right panel, corresponding autocorrelation functions. L_c = 1.75 km, S = -4, σ^2 = 1.02E-03, spacing = 100 m. Unmodified theoretical autocorrelation function. Six predictor coefficients

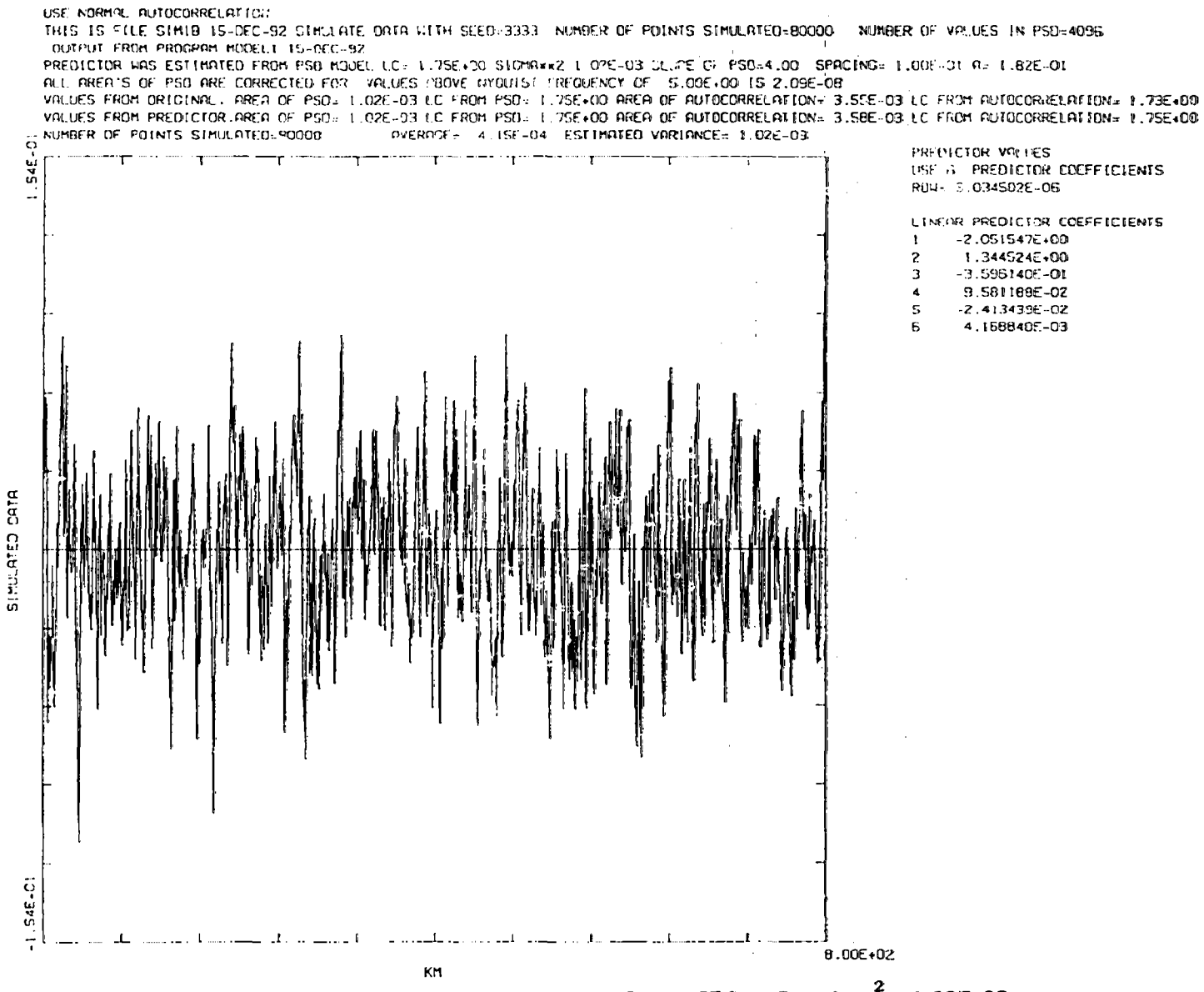

Figure 30. Autoregressive simulated structure sequence. L_c = 1.75 km, S = -4, σ^2 = 1.02E-03

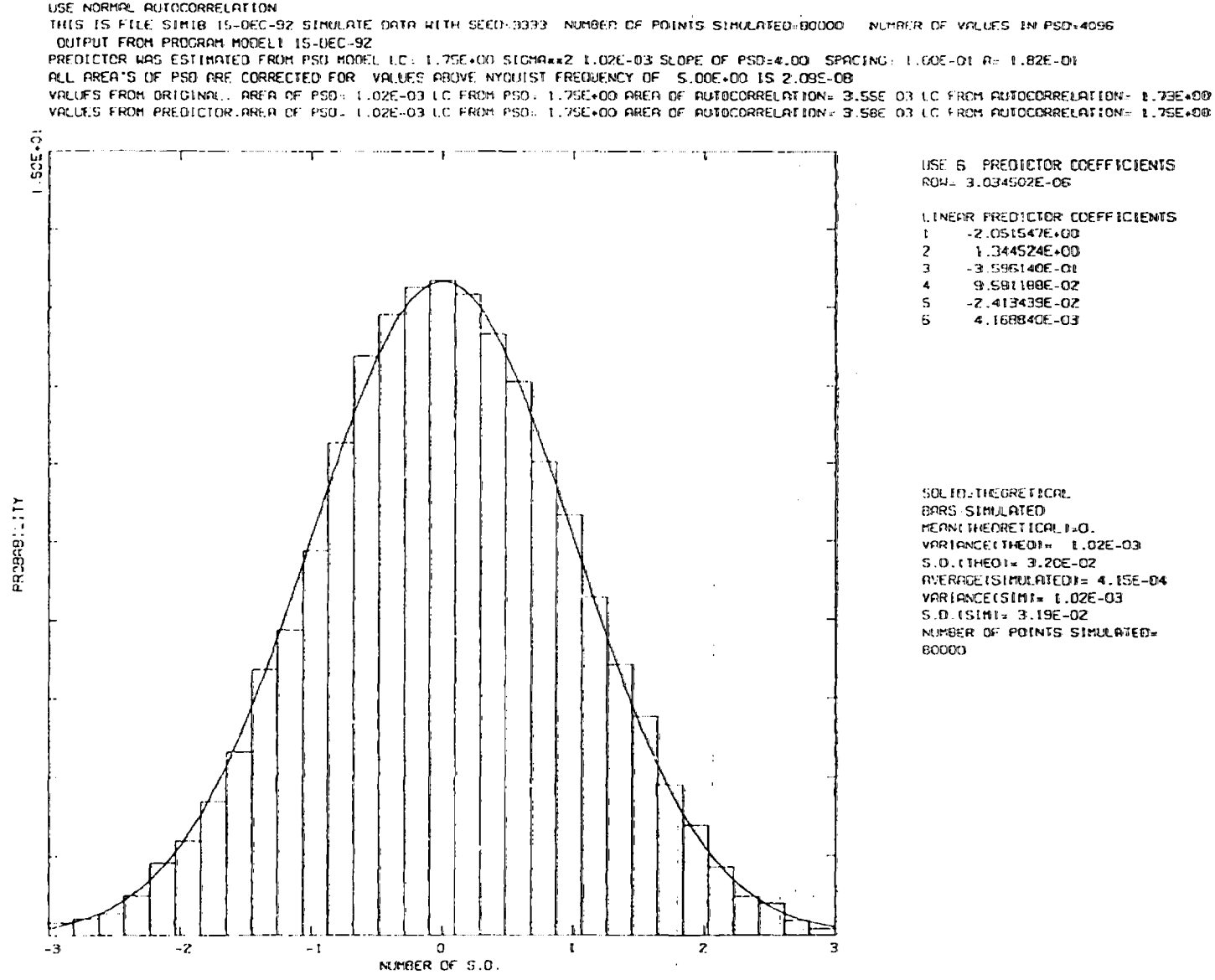

Figure 31. Histogram of autoregressive simulated structure sequence. L_c = 1.75 km, S = -4, σ^2 = 1.02E-03

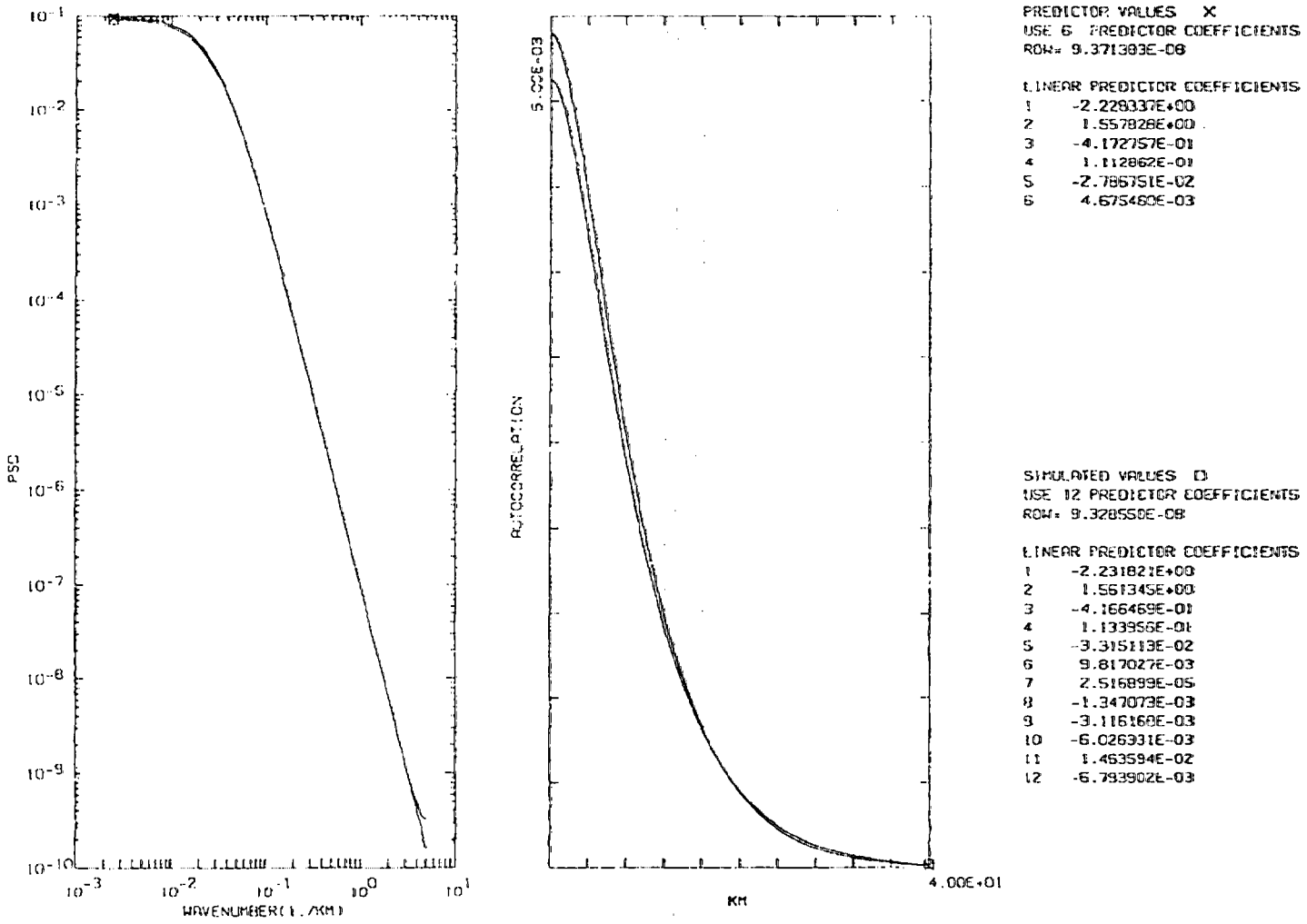

Figure 32. Left panel, theoretical PSD input (unmarked), autoregressive predictor PSD (marked by x), and simulated PSD (marked by small square). Right panel, corresponding autocorrelation functions. L_c = 10 km, S = -4, σ^2 = 4.9E-03, spacing = 100 m. Unmodified theoretical autocorrelation function. Six predictor coefficients

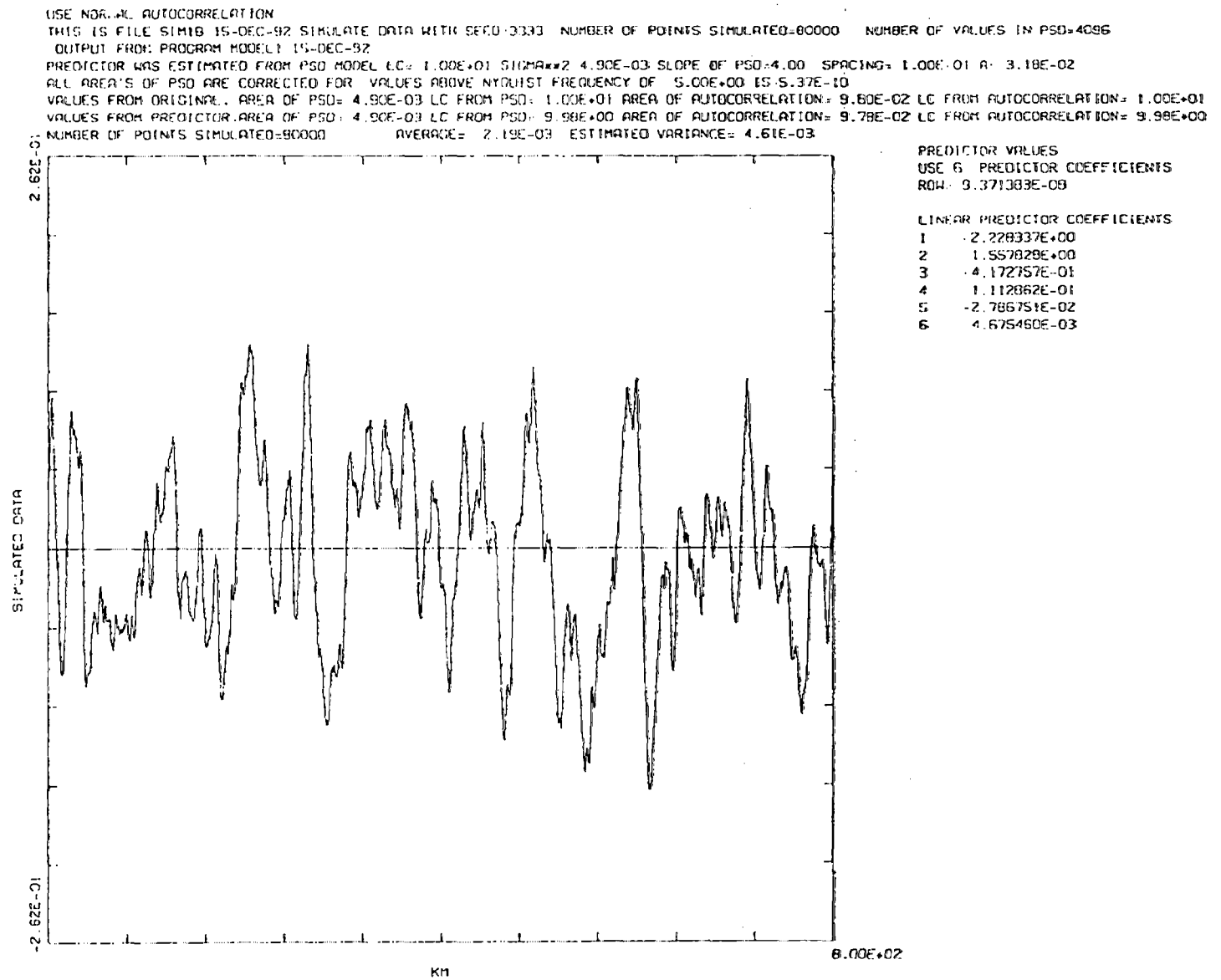

Figure 33. Autoregressive simulated structure sequence. L_c = 10 km, S = -4, σ^2 = 4.9E-03

USE NORMAL AUTOCORRELATION
THIS IS FILE SIM1B 15-DEC-92 SIMULATE DATA WITH SEED=3033 NUMBER OF POINTS SIMULATED=80000 NUMBER OF VALUES IN PSD=4096
OUTPUT FROM PROGRAM MODEL1 15-DEC-92
PREDICTOR WAS ESTIMATED FROM PSD MODEL LC= 1.00E+01 SIGMA**2 4.90E-03 SLOPE OF PSD=4.00 SPACING= 1.00E-01 A= 3.18E-02
ALL AREA'S OF PSD ARE CORRECTED FOR VALUES ABOVE NYQUIST FREQUENCY OF 5.00E+00 IS 5.37E-10
VALUES FROM ORIGINAL, AREA OF PSD= 4.90E-03 LC FROM PSD= 1.00E+01 AREA OF AUTOCORRELATION= 9.80E-02 LC FROM AUTOCORRELATION= 1.00E+01
VALUES FROM PREDICTOR.AREA OF PSD= 4.90E-03 LC FROM PSD= 9.98E+00 AREA OF AUTOCORRELATION= 9.78E-02 LC FROM AUTOCORRELATION= 9.98E+00

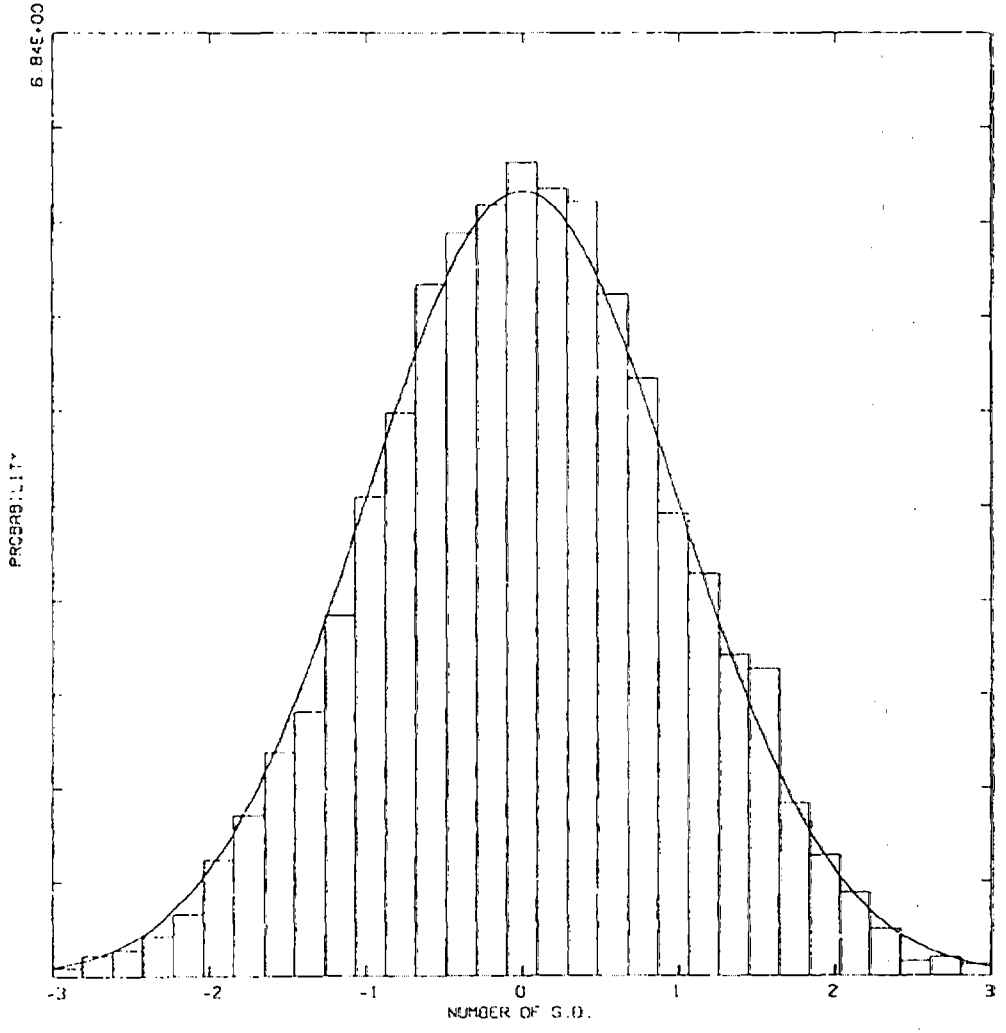

USE 6 PREDICTOR COEFFICIENTS
ROH= 9.371383E-08

LINEAR PREDICTOR COEFFICIENTS
1 -2.228337E+00
2 1.557828E+00
3 -4.172757E-01
4 1.112862E-01
5 -2.786751E-02
6 4.675460E-03

SOLID=THEORETICAL
BARS=SIMULATED
MEAN(THEORETICAL)=0.
VARIANCE(THEO)= 4.90E-03
S.D.(THEO)= 7.00E-02
AVERAGE(SIMULATED)= 2.19E-03
VARIANCE(SIM)= 4.61E-03
S.D.(SIM)= 6.79E-02
NUMBER OF POINTS SIMULATED=
80000

Figure 34. Histogram of autoregressive simulated structure sequence. L_c = 10 km, S = -4, σ^2 = 4.9E-03

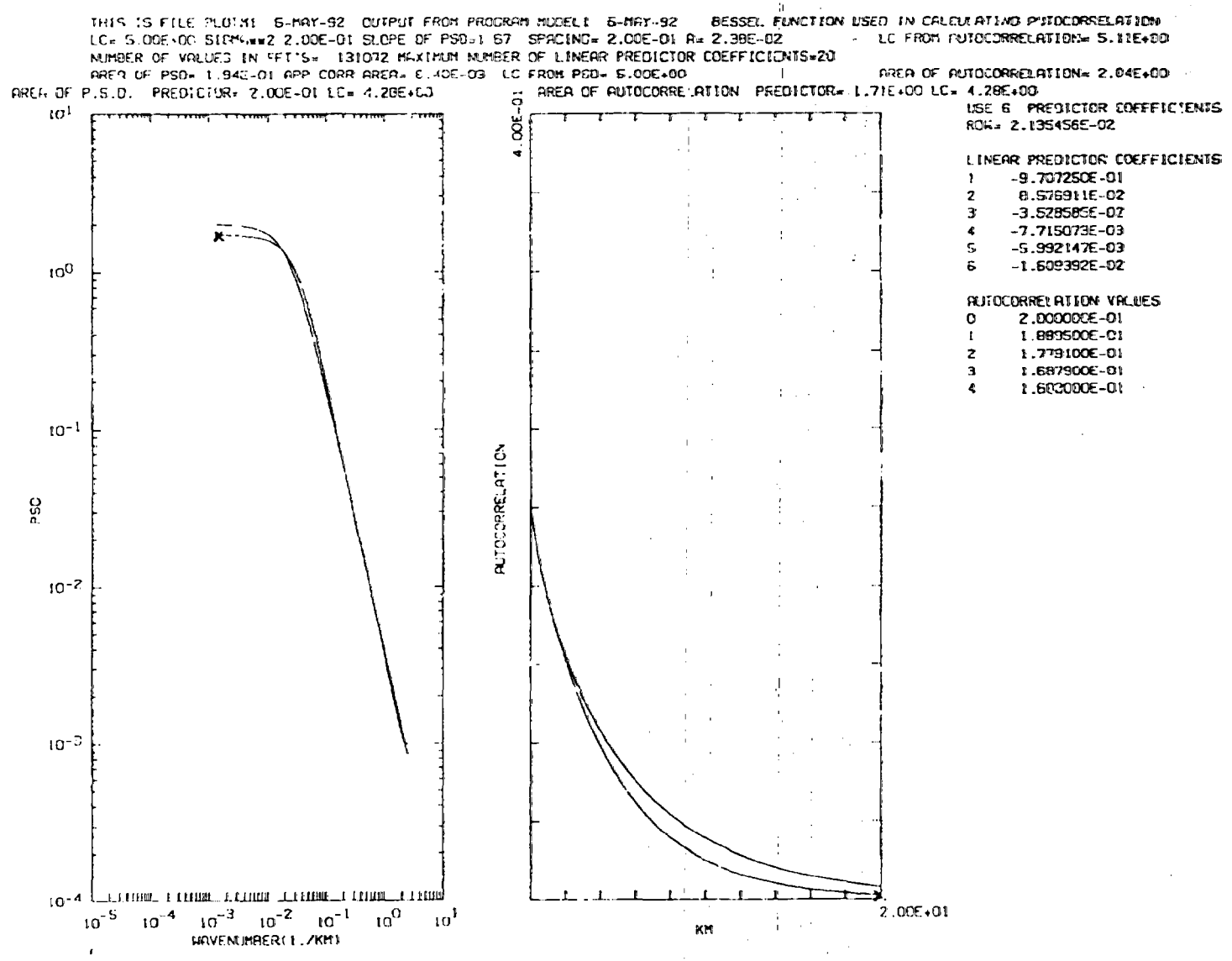

Figure 35. Left panel, theoretical PSD input (unmarked), autoregressive predictor PSD (marked by x). Right panel, corresponding autocorrelation functions. L_c = 5 km, S = -5/3, spacing = 200 m. Theoretical autocorrelation function modified at lag = 0. Six predictor coefficients

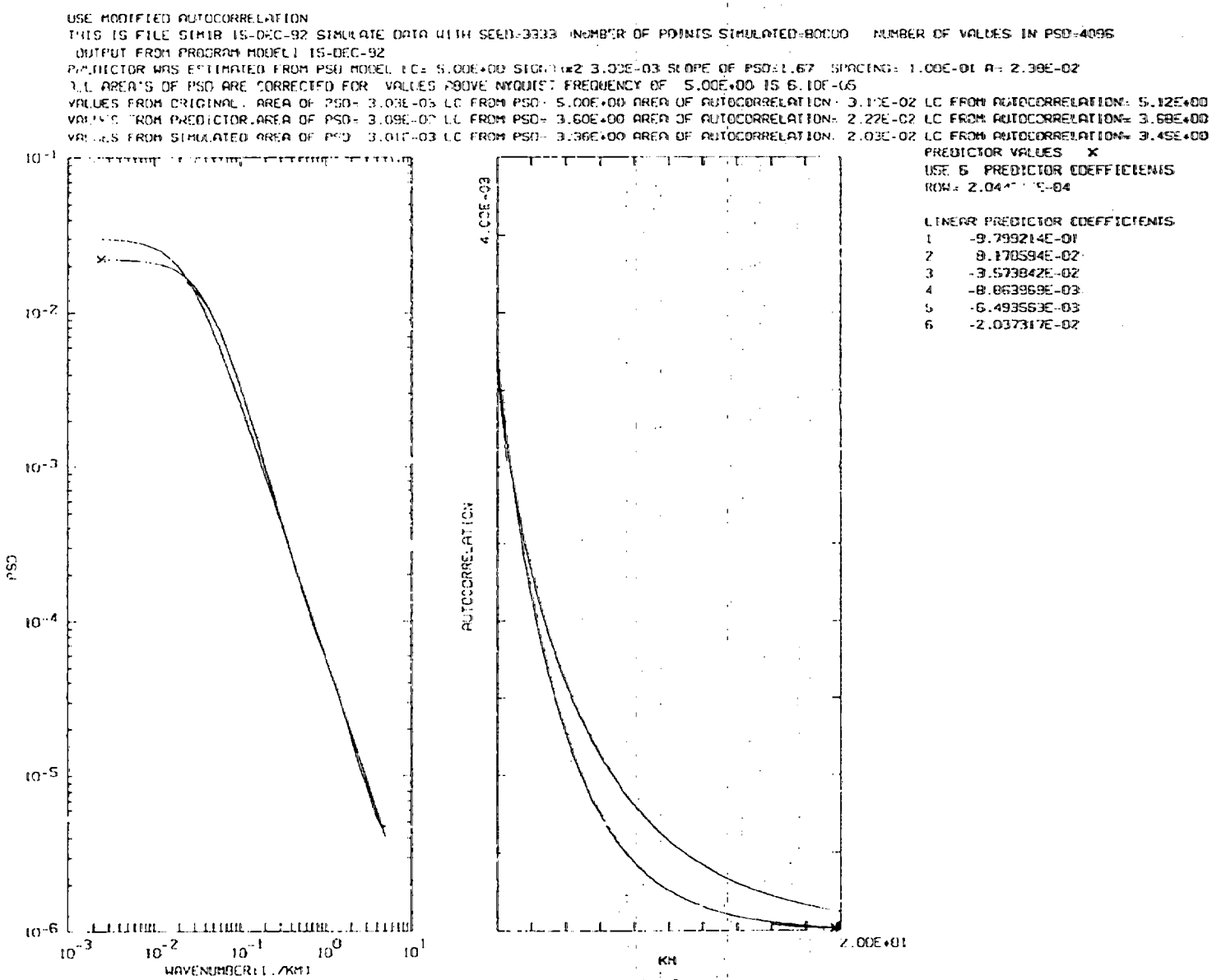

Figure 36. Left panel, theoretical PSD input (unmarked), autoregressive predictor PSD (marked by x). Right panel, corresponding autocorrelation functions. L_c = 5 km, S = -5/3, spacing = 100 m. Theoretical autocorrelation function modified at lag = 0. Six predictor coefficients

References

1. Sharma, R.D., Duff, J.W., Sundberg, R.L., Gruninger, J.H., Bernstein, L.S., Robertson, D.C., and Healey, R.J. (1991) *Description of SHARC-2, The Strategic High Altitude Atmospheric Radiance Code*, Phillips Laboratory technical report PL-TR-91-2071, ADA 239008
2. Marple, S. L., (1987) *Digital Spectral Analysis with Applications*, Chapter 6, Prentice-Hall, Englewood Cliffs, New Jersey.
3. Kay, Steven M., (1988) *Modern Spectral Estimation, Theory & Application*, Prentice-Hall, Englewood Cliffs, New Jersey.
4. Tatarski, V.I., (1961) *Wave Propagation in a Turbulent Medium*, McGraw-Hill, New York.
5. Futterman, W.I., Schweitzer, E.L., and Newt, J.E. (1991) Estimation of Scene Correlation Lengths, *Characterization, Propagation, and Simulation of Sources and Backgrounds, Proceedings SPIE* - The International Society of Optical Engineering, V1486, pp127-140, Orlando, Florida.
6. For the integral, see for example, Gradshteyn, I.S. and Ryzhik, I.M., *Table of Integrals Series and Products*, eq 3.241.4, Academic Press, 1965.
7. Ibid., eq 8.432.5
8. Bracewell, R.N., (1978) The Fourier Transform and Its Applications, McGraw-Hill, New York.
9. Ibid.
10. Haykin, Simon, ed., (1991) *Advances in Spectrum Analysis and Array Processing*, Vol. I, Prentice Hall, Englewood Cliffs, New Jersey, pp.155-156.
11. Strugala, L.A., Newt, J.E., Futterman, W.I., Schweitzer, E.L., Herman, B.J., and Sears, R.D., (1991) Development of High Resolution Statistically Non-stationary Infrared Earthlimb Radiance Scenes, *Characterization, Propagation, and Simulation of Sources and Backgrounds, Proceedings SPIE* - The International Society for Optical Engineering, V1486, pp.176-187, Orlando, Florida.

Appendix

Extensions of AR Methods to Non-Stationary Data and to Two and Three Dimensions

A1. NON-STATIONARY DATA

The methods employed here easily can be extended to simulate a non-stationary discrete spatial series. If L_c, σ^2, or spectral slope are allowed to vary slowly, sets of a_i^k coefficients and associated σ_k^2 values for each point k can be evaluated, where a_i^k is the i^{th} coefficient at point k with the simulated results starting at k = 1. Y(k) can then be simulated by setting Y(-L) = Y(-L+1) = Y(L+2) = ··· = Y(-L+N-1) = 0 (where L is some number, say 100, and N is the number of coefficients). With k = -L+N, -L+N+1, ···, 1, the iterative expression for Y(k) is:

$$Y(k) = \sigma_1 G(k) - \sum_{i=1}^{N} a_i^1 Y(k-i)$$

and for k > 1, Y(k) is:

$$Y(k) = \sigma_k G(k) - \sum_{i=1}^{N} a_i^k Y(k-i)$$

A2. TWO AND THREE DIMENSIONAL SIMULATIONS

The methods employed in the text can be extended to simulate horizontal and vertical data. Assume we wish to simulate data at altitudes k = 1, 2, ···. Then using either a Fourier transform method or the linear prediction technique, one may form a simulated sequence whose horizontal PSDs are the PSD from the L_c and slope at each horizontal altitude with σ set to 1. In addition, one must form simulated values at altitudes -L, -L+1, ···, 0 from L_c and slope (horizontal) for k = 1

and for σ set to 1. Let us call the resulting values $Z(k,j)$ where k is the altitude and j is a point number (j could represent a point on a horizontal line or, by extension, a point in a two-dimensional horizontal sheet). Then the final data having the desired horizontal and vertical PSD's, $F(k,j)$, is formed by filtering $Z(k,j)$ as follows.

For $k = -L, -L+1, -L+2, \cdots, 1$

$$F(k,j) = \sigma_1 Z(k,j) - \sum_{i=1}^{N} a_i^1 Z(k-i,j)$$

where σ_1 and a_i^1 are the values found using the Levinson algorithm with r_{xx} determined from σ and the vertical values of L_c and slope at altitude =1.

Then for $k > 1$,

$$F(k,j) = \sigma_k Z(k,j) - \sum_{i=1}^{N} a_i^k Z(k-i,j)$$

where σ_k and a_i^k are the values found using the Levinson algorithm with r_{xx} determined from σ and the vertical values of L_c and slope at altitude k.

In the above analysis, it should be noted that with careful programming only N+1 altitudes need to be stored at any time during the computations. This can reduce the necessary storage by a factor of 10 or more.